Female bone physiology resilience in a past Polynesian outlier community

Justyna J. Miszkiewicz[1,2]*, Hallie R. Buckley[3], Michal Feldman[4,5,6], Lawrence Kiko[7], Selina Carlhoff[6], Kathrin Naegele[6], Emilie Bertolini[8], Nathalia R. Dias Guimarães[1], Meg M. Walker[1], Adam Powell[9], Cosimo Posth[4,5,6], Rebecca L. Kinaston[3,10,11]

[1]School of Archaeology and Anthropology, Australian National University, Canberra, Australia
[2]School of Social Science, University of Queensland, St Lucia, Australia
[3]Department of Anatomy, Otago School of Biomedical Sciences, University of Otago, Dunedin, New Zealand
[4]Archaeo- and Palaeogenetics Group, Institute for Archaeological Sciences, University of Tübingen, Tübingen, Germany
[5]Senckenberg Centre for Human Evolution and Palaeoenvironment, University of Tübingen, Tübingen, Germany
[6]Department of Archaeogentics, Max Planck Institute for Evolutionary Anthropology, Leipzig, Germany
[7]The Solomon Islands National Museum, Honiara, Solomon Islands
[8]Department of Archaeogentics, Max Planck Institute for the Science of Human History, Jena, Germany
[9]Department of Human Behavior, Ecology and Culture, Max Planck Institute for Evolutionary Anthropology, Leipzig, Germany
[10]Centre for Social and Cultural Research, Griffith University, Queensland, Australia
[11]BioArch South, Waitati, New Zealand

*CORRESPONDENCE: j.miszkiewicz@uq.edu.au (ORCID: 0000-0002-9769-2706)

1 **ABSTRACT**

2 Remodelling is a fundamental biological process involved in the maintenance of bone

3 physiology and function. We know that a range of health and lifestyle factors can impact this

4 process in living and past societies, but there is a notable gap in bone remodelling data for

5 populations from the Pacific Islands. We conducted the first examination of femoral cortical

6 histology in 69 individuals from ca. 440-150 Taumako in Solomon Islands, a remote

7 'Polynesian Outlier' island in Melanesia. We tested whether bone remodelling indicators

8 differed between age groups, and biological sex validated using ancient DNA. Bone vascular

9 canal and osteon size, vascular porosity, and localised osteon densities, corrected by femoral

10 robusticity indices were examined. Females had statistically significantly higher vascular

11 porosities when compared to males, but osteon densities and ratios of canal-osteon (~8%) did

12 not differ between the sexes. Our results indicate that, compared to males, localised femoral

13 bone tissue of the Taumako females did not drastically decline with age, contrary to what is

14 often observed in modern populations. However, our results match findings in other

15 archaeological samples—a testament to past female bone physiology resilience, also now

16 observed in the Pacific region.

INTRODUCTION

19

20 Peak bone mass attainment in modern humans occurs around the third life decade and is

21 marked by a striking sex-specific difference whereby biological females (hereafter 'females')

22 typically accrue less bone than biological males (hereafter 'males') [1,2,3]. Bone density

23 becomes further compromised around the fifth-sixth life decade when females experience

24 menopause and a significant reduction in the osteoclast inhibiting estrogen [4,5,6]. The

25 physiological maintenance of bone throughout the life-course is executed by remodelling, a

26 process sensitive to a range of internal and external stimuli [7]. Bioarchaeological research on

27 human skeletal remains with well-preserved bone microstructure has provided data on bone

28 remodelling under a range of cultural and environmental conditions [8,9,10,11,12]. However,

29 there is a notable gap in data for past populations from across the Pacific Islands, except for

30 two recent studies that used small samples sizes quantifying bone vascular porosity in eight

31 individuals from Tonga [13], and comparing bone histology between the femur, rib, and

32 humerus in one individual from the Marshall Islands [14]. Here, we report the first adult

33 human femur quantitative bone histology data for an archaeological 'Polynesian Outlier'

34 skeletal assemblage from a ca. 750–300 BP site on Taumako, Southeast Solomon Islands [15,

35 16, 17] (Figure 1).

36

37 There are several reasons why bone remodelling in the past inhabitants of Taumako is worth

38 investigating. The Solomon Islands are part of Oceania, which is a region with complex

39 migration histories [18]. Taumako Island, despite being located in Near Oceania, is known as

40 a 'Polynesian Outlier' (i.e. part of Polynesia) due to a purported blow-back migration of

41 populations from Polynesia during the mid-second millennium AD, and where Polynesian is

42 the main language today [19]. Human mobility between different regions, including islands

43 from Melanesia, Micronesia, and Polynesia, facilitated an exchange of cultural practices but

44 also encouraged spread of diseases [19, 20]. A notoriously high incidence of metabolic and

45 infectious conditions is widespread across the Pacific Islands, particularly in Near Oceania,

46 evidence for which has come from modern epidemiological research and studies of disease in

47 archaeological human remains [21, 22]. For the Taumako archaeological remains

48 specifically, skeletal lesions indicative of endemic yaws and iron-deficiency anaemia

49 (potentially exacerbated by high malaria pathogen loads) have been noted [23, 24, 25]. This

50 is in addition to large variation in stature, age- and sex- specific dietary practices relating to

51 social status [17, 20, 26], and tendency for males to die younger than females at Taumako

52 when compared with neighbouring Tonga in western Polynesia [23, 24]. All of these findings

53   suggest experiences of population-wide physiological stress at Taumako. As we do not yet

54   have bone remodelling data for this archaeological sample, we do not understand how, and if,

55   bone growth varied across this population, or whether it was influenced by these experiences

56   of physiological stress. The aim of our study is to report baseline bone remodelling data for

57   Taumako, which will add new insights into the current limited knowledge about past human

58   bone physiology across Pacific Island habitats. Our data will expand understanding of bone

59   growth dynamics within spatially and temporally distributed archaeological populations, and

60   might be of interest to the International Osteoporosis Foundation, which is currently mapping

61   the occurrence of fractures across the Asia-Pacific region [27].

62

63   **Bone remodelling through human life-course**

64   Based on bone mineral density (BMD) and fracture incidence data, it is established that

65   significant bone loss occurs with age [28, 29]. Bone building capacities in early adulthood

66   play a key role in determining the rate at which bone metabolic activity becomes out of

67   balance later in life [2]. While early life skeletal mass accrual is largely genetically

68   determined, other factors such as physical activity, diet, and lifestyle habits, can also impact

69   bone metabolism [12, 30]. Generally, there are three key areas that characterise bone mass

70   change in modern humans—peak bone mass accrual in the third life decade, drastic bone loss

71   after menopause in females, and significant bone loss in both sexes in old age [2]. The first

72   three life decades are spent creating a 'bone bank' that is used for the remainder of the life-

73   course [31]. The female preponderance of bone loss is due to life-course variability in

74   estrogen levels, which inhibit prolonged bone resorption [4]. The effect of menopause on

75   bone health can be mediated through lifestyle factors and calcium supplements available to

76   women today. Modern clinical techniques can diagnose osteoporotic bone from BMD T-

77   scores [32] and bone remodelling histological markers to check whether osteoclast-mediated

78   bone resorption outweighs bone deposition by osteoblasts.

79

80   While BMD has been previously examined in some archaeological samples (see reviews in

81   [8-12, 33]), histological characteristics of cortical remodelling assessed from thin sections by

82   histomorphometric and histomorphological methods have also been successfully evaluated

83   [34, 35]. Cortical bone not only experiences metabolic turnover events that ensure suitable

84   calcium reservoirs, it also responds to biomechanical stimuli that drive bone cell activity [7].

85   As teams of osteoblasts and osteoclasts execute bone remodelling as part of Bone

86 Multicellular Units (BMUs) that travel through the cortex, they leave behind remodelling

87 products of circular structure—secondary osteons (hereafter 'osteons')—that can be studied

88 histologically, and thus offer an insight into bone remodelling activity in an individual [36].

89 The area of osteons and Haversian canals within these can aid in determining whether a

90 typical BMU formed over relatively longer or shorter periods of time, whereby larger osteons

91 simply fill more space in bone (though this depends on the ratio of lamellar bone to

92 Haversian canal in individual osteons) [37, 38, 39, 40]. Osteons are also replaced by

93 subsequent generations of osteons, creating a total population of remodelled bone per given

94 region [40], whereas the densities of vascular pores (Haversian canals, Volkmann's canals,

95 primary/simple vessels) reflect the complex interconnected network cortical bone uses to

96 circulate blood and interstitial fluid containing oxygen and nutrients important for bone

97 homeostasis [41, 42].

98

99 **Bone remodelling in archaeological humans**

100 In cases of archaeological human bone that is well preserved microstructurally, studies have

101 been able to reconstruct bone remodelling capacities and link them to aspects such as gender

102 division of labour and sex-specific bone remodelling [43], changes in subsistence strategies

103 through time [44], or medieval lifestyles associated with socio-economic disparities [45]. For

104 example, Mulhern and Van Gerven [43] found higher osteon densities in femoral cross-

105 sections of males than females from Medieval Sudanese Nubia, but no sex differences in

106 Haversian canal dimensions, suggesting sex-specific activities with physically strenuous tasks

107 of males contributing to the observed remodelling patterns. Miszkiewicz et al [13] found

108 severely porous Haversian bone in adult females compared to denser bone samples of males

109 from 2,650 BP Tonga, indicating experiences of abnormal bone loss likely related to both age

110 and activity. However, bioarchaeological studies where bone remodelling has been

111 investigated through histological means have also cautioned that we do not yet fully

112 understand the spectrum of bone histology parameters manifested in archaeological samples

113 [46], and that relying on very specific interpretations (e.g. behaviour) made from histological

114 data is clouded by multiple other confounding variables [47] such as health, nutrition,

115 ancestry and individual or population-based variations in metabolic activity. Therefore,

116 interpretations of archaeological human bone histology data are usually context specific.

117 However, with an increasing number of sites/collections reported, we may be able to start

118 building a better understanding of possible changes in bone remodelling through time and

119 space in recent humans. For example, one prior analysis comparing tibial and femoral bone

120 histology between Pleistocene specimens (including Broken Hill, Shanidar 2, 3, 4, 5, 6,

121 Tabun 1, and Skhul 3, 6, 7) and a pre-Columbian Pecos human sample, reported similar

122 levels of bone remodelling characterising the two [48], but smaller size of osteonal structures

123 in the Pleistocene sample [49].

124

125 As bone histology research using archaeological samples gathers increasing amounts of data,

126 it is apparent that a significant gap remains for populations from across the Asia-Pacific

127 region. While access to large samples of human remains is limited in the remote areas of the

128 Pacific, excavation on Taumako Island in the southeast Solomon Islands produced one of the

129 largest well-preserved skeletal samples in the region [15]. Study of this skeletal assemblage

130 presents an excellent opportunity for bone remodelling research.

131

132 Modern Pacific Island nations, particularly in Polynesia, are impacted by widespread

133 metabolic syndrome related conditions, including type 2 diabetes and obesity [21].

134 Archaeological evidence demonstrates the occurrence of gout and diffuse idiopathic skeletal

135 hyperostosis, as well as infectious and nutritional conditions affecting health from the time of

136 first settlement ca 3,000 BP in Remote Oceania (the islands east of the Solomons chain) [21,

137 50, 51, 52]. Island environments are associated with food shortages, climate and

138 environmental instability, affecting health in the past and today [21, 50, 53]. Long-term

139 exposure to pathogens, and population admixture prior to, and crossing-over with, the

140 European contact in the 16th-17th centuries could be reflected in community-specific bone

141 remodelling capacities as an adaption to endemic disease and society specific structures that

142 determine diet and society roles. For example, one prior study of 61 Taumako individuals

143 recorded cortical bone indices of the metacarpal and femur, in addition to femur length, to

144 find that no distinct stress or functional adaptation signal could be detected specifically as a

145 result of island conditions [54]. However, this study did not collect microscopic bone data—a

146 gap which our study will fill.

147

148 Given the significance of archaeological human samples in improving modern bone biology

149 research, the Pacific Island gap in our knowledge relating to archaeological bone

150 remodelling, and the island environmental context of the Solomon Islands, this study tested

151 whether (1) femur bone histology from archaeological Taumako males and females showed

152   differences in remodelling and tissue organisation indicators, and (2) to what extent these

153   bone microstructure features changed with age. Our total sample size was 69 (33 males and

154   36 females). We selected the posterior midshaft femur because of its biomechanical

155   versatility reflecting sex-specific lifestyles and sexual dimorphism, which we first evaluated

156   in this sample through basic gross measures of femoral size (midshaft circumference, cortical

157   width, maximum length [54]) and robusticity indices [55] computed from these values. Next,

158   we created thin sections from which we measured standard static histological variables

159   (vascular canal and osteon area to compute canal-osteon ratios [56], and localised osteon

160   density [40]) as proxies for bone remodelling activity, and vascular porosity as a proxy for

161   bone blood supply and reflecting bone tissue organisation [41]. Histology was examined in

162   intra-cortical, and combined (including periosteal and endosteal areas) cortical regions of

163   interests (ROIs) of the thin sections (Figure 2). The femoral size data were then used to adjust

164   histology data to account for microscopic-macroscopic scaling issues, and within-sample

165   variation stemming from inherent bone size differences between males and females. We then

166   compared the data between male and age groups.

167

168   We hypothesised indicators of higher bone resorption over formation should be evident in

169   females when compared with males, and in older individuals when compared with those of

170   younger age. Our age and sex estimates are based upon standard gross anatomy methods,

171   which assess age-progressive and sexually dimorphic skeletal landmarks of the skull, teeth,

172   and the pelvis [57, 58]. Our sex estimates were validated by determining XY or XX

173   karyotypes via ancient DNA (aDNA), yielding 88% of successful sex matching through these

174   two methodological approaches. This study can only treat sex as a biological trait and cannot

175   consider gender identity which is unknown for these Taumako individuals. We present

176   analyses based on skeletal sexual dimorphism and genetic information within the limits of

177   our sample and available context, but we recognise that many biological traits associated with

178   sex are not binary and exist on a spectrum [59].

179

180   **RESULTS**

181   Sexual dimorphism manifested in size variation across the Taumako femora. The Taumako

182   males had ($p < 0.001$, Tables 1-3) larger femoral midshafts and thicker posterior cortical

183   walls (average circumference = 95.79 mm, average cortical width = 10.77 mm) compared to

184   females (average circumference = 89.81 mm, average cortical width = 8.77 mm). Females

185   also had slightly shorter femora than males, though this difference was not tested statistically

186   due to a small sub-sample size (n = 23) of the individuals with intact femora. Robusticity

187   indices (unitless values) calculated based upon midshaft circumference and cortical width

188   were greater in males (average circumference robusticity = 22.85; average cortical width

189   robusticity = 2.58) when compared to females (midshaft circumference robusticity = 20.66,

190   cortical width robusticity = 2.08), but could not be validated using statistical tests either

191   because they were based on the limited femoral length data. We could not apply age related

192   inferential statistical tests to the gross morphometric femoral data, except for circumference

193   and cortical width, which did not change statistically across any of the age classes in the

194   whole sample ($p > 0.05$, Table 1). Within females and males, there was no age effect on

195   midshaft circumference or cortical width either. Given that some of the gross femoral

196   measurements varied with sex (likely because males have larger femora than females in our

197   sample) adjustments of bone histology data by femoral size were necessary [60, 61].

198

199   **Femoral vascular porosity and bone remodelling indicators at Taumako**

200   Looking at descriptive statistics only, vascular porosity, canal-osteon ratios, and osteon

201   densities were greater in females when compared to males (Table 2). When applying inferential

202   statistical tests, out of all three variables, vascular porosity in females adjusted (unitless values)

203   by both cortical width (average vascular porosity adjusted by cortical width = 2.34) and

204   midshaft circumference (average vascular porosity adjusted by midshaft circumference =

205   22.02) were statistically significantly higher ($p < 0.0001$) than in males (average vascular

206   porosity adjusted by cortical width = 1.64, average vascular porosity adjusted by midshaft

207   circumference = 18.34) (Table 3, Figure 3). However, the vascular canal-osteon ratios did not

208   differ statistically between the sexes ($p > 0.05$, Tables 2, 3), with both sub-groups bordering an

209   approximate 8% (averages of 7.61% in males and 8.31% in females). We did not attempt an

210   inferential statistical comparison of the osteon density data, and on further sub-divisions by age

211   due to inadequately small sample size in the sub-groups (Table 2).

212

213   Secondly, there was a clear change in the descriptive statistics of bone histology values from

214   young to old individuals whereby all peaked in the middle-age category (Tables 2, 3, Figure

215   3). While all the histology data were lower in the young or old age sub-groups when

216   compared to the middle-age sub-group, the old individuals showed the lowest values across

217   the entire sample with the exception of canal-osteon ratios which were slightly higher.

218   However, none of these changes with age, apparent when considering the data means, were

219   statistically significant ($p > 0.05$) (Table 3). As above, we did not attempt an inferential

220 statistical comparison of the osteon density data, or on further sub-divisions by sex due to

221 inadequately small sample size in the sub-groups (Table 2). Collectively, our results partly

222 support our hypothesised expectations.

223

224   **DISCUSSION**

225 Our age and sex analyses of the Taumako bone histology data revealed that the Taumako

226 females had higher vascular porosity of their femoral cortical bone compared to males, while

227 intra-cortical variables of osteon densities and canal-osteon area ratios did not differ

228 statistically significantly between the sexes. This occurred despite males and females having

229 sexually dimorphic femora at Taumako. A possible isometric effect of larger male femur size

230 on bone histology can be excluded as underlying these results as our data were corrected by

231 femoral midshaft size measures and robusticity indices [60, 61]. Acknowledging small

232 sample size in some of the age and sex sub-groups, and with the data at hand, we will discuss

233 possible implications of our results for adult femur bone physiology at Taumako.

234

235   **Sex and cortical bone histology at Taumako**

236 The femoral samples of Taumako females were more vascularised than those of males. We

237 will not link this to bone remodelling only [42], because our data for the vascular porosity are

238 made up of Haversian canals with the possibility of including some primary vessels (see

239 Materials and Methods). This is a result of us accounting for localised diagenesis apparent in

240 the thin sections. Therefore, this measure is that of an accumulation of vascular cavities up

241 until the point of death, rather than just reflecting recent remodelling events, and we cannot

242 be sure which canals had been replaced in the first few life decades in these individuals.

243 Further, the vascular porosity data stem from the posterior femur 'strip' region overlapping

244 an entirety of compact bone, so the porosity counts reflect our inclusion of both the periosteal

245 and endosteal bone regions where there might have been region-specific variation in pore

246 counts. Our main interpretation is that the higher densities of vascular pores in females

247 suggest their bones received greater blood and nutrient supply than that of males [42]. Male

248 frailty due to endemic disease, inferred from their younger mortality compared to females at

249 Taumako [16, 26], may have contributed to this bone characteristic, which we discuss further

250 below. Despite the greater density of cortical pores in females, neither the osteon population

251 density nor the geometric properties of secondary osteons differed statistically between the

252   sexes. The ratio relationship between Haversian canals and osteon area was almost the same

253   when comparing the sexes (approximately 8%). We expected higher Haversian canal area in

254   females than males indicating prolonged osteoclast-mediated bone resorption. This suggests

255   that the intra-cortical midshaft femoral bone in Taumako males and females experienced

256   similar remodelling events.

257

258   Prior bioarchaeological research reported inconsistencies in osteon morphometry when

259   comparing the sexes similar to those we present for Taumako. For example, data for males in

260   the Medieval Sudanese sample, mentioned in our Introduction, showed higher osteon

261   densities than in females, but females had larger osteons than males [43]. However, similar to

262   us, Mulhern and Van Gerven [43] reported a lack of statistically significant differences in the

263   geometric properties of Haversian canals between the sexes. Similarly, 14th-19th centuries

264   Pecos females (New Mexico) had relatively large secondary osteons, but with smaller

265   Haversian canals when compared to males [62]. Burr et al. [62] observed a lack of distinct

266   bone loss in the Pecos females, citing a physically active lifestyle as a possible factor driving

267   the maintenance of good bone density. In the 700 BC to 19th century Canadian Baffin Island

268   male and female skeletons, no significant differences were noted when considering the

269   density of Haversian canals and the area of secondary osteons [63]. As noted by Pfeiffer [46],

270   there is a clear variability in how bone histology is expressed in archaeological populations,

271   as illustrated by the above examples, complicating inter-population comparisons. A

272   Taumako-specific approach is needed to contextualise our results.

273

274   Outside of a genetic basis to the morphology of adult compact bone, the Taumako femoral

275   bone histology could reflect a combination of the following population-specific factors: the

276   socio-economic make-up and diet of the community, and the effect of physiological stress

277   and disease on skeletal development. Having studied grave goods (including shell money,

278   bobbles, and Tridacna shell 'tavi' neck ornaments) from across the Taumako burials,

279   archaeologists have previously determined that this community was stratified into status

280   groups on the basis of wealth and inherited rank [15]. Leach and Davidson [15] quantified the

281   value of grave goods finding that the Tridacna breast pendants were the most prestigious.

282   Kinaston et al. [17] used this information to test for status-related access to food in 99 of

283   Taumako individuals. They [17] analysed carbon, nitrogen, and sulfur stable isotopes in bone

284   collagen to confirm that wealthy Taumako individuals ate high status foods consisting of high

285 trophic level animals such as pigs, fish, and turtles. This was the case for both high status
286 males and females. However, all wealthy individuals, and all males, overall, had elevated
287 levels of nitrogen when compared to low status females. In our study, at least 15 (~22%)
288 individuals were of very high status (Leach and Davidson [15] used a 'wealth index'),
289 including nine males and six females, with seven males and five females being buried with
290 the prestigious Tridacna breast pendants. The combination of mixed-sex individuals who
291 regularly fed on high protein foods, and others who fed on lower ranking foods or
292 experienced nutritional stress (see below), could have resulted in the balanced osteon density
293 and canal-osteon areas across the sexes. This mirrors prior research comparing high and low
294 social status human bone histology in medieval England where upper-class foods were
295 associated with higher osteon densities in the femur [45, 64].

297 In addition, the lack of intra-cortical remodelling differences between the sexes, but lower
298 vascular porosity in males, could be explained through Taumako male frailty. Kinaston and
299 Buckley [16] used carbon and nitrogen stable isotopes in bone collagen and tooth dentine to
300 infer that nutritional stress led to early deaths of some adolescent and young males at
301 Taumako. This was also found by Stantis et al [26] who examined nitrogen stable isotopes in
302 tooth dentine in this sample. Combined with the long history of malaria and yaws exposure at
303 Taumako, experiences of inconsistent dietary intake in lower ranking adolescents might have
304 led to poor bone maintenance later in life [65] (males are considered to be more susceptible to
305 physiological stress than females because sex-steroids regulate immune response [66, 67]).
306 Also, in some indigenous Solomon Island populations today, growth and nutritional status of
307 females is reported to be much better than that of young males [68]. Even though no sex-
308 specific differences in gross anatomical markers of stress, such as linear enamel hypoplasia or
309 lesions indicative of yaws, have been previously noted in the Taumako assemblage [24, 69],
310 our bone histology data offer a microscopic perspective which is a proxy for repetitive,
311 longer-term bone physiological cycles. Thus, we infer that Taumako females might have been
312 equipped with dense intra-cortical femoral bone to buffer excessive bone loss. We know from
313 experimental research that loss of calcium is compensated for by increasing remodelling in
314 lactating females, which ultimately restores compromised bone tissue during reproduction
315 [70, 71].
316   **The effect of age on bone histology at Taumako**

317   Two key areas of concern to life-long human bone building capacities are the third and fifth-

318   sixth decades reflecting peak bone mass accrual and female menopause, respectively [2].

319   Bone mass in modern humans through the life-course is easier to map than in past

320   populations as we cannot observe life-long change to bone mass accrual in the archaeological

321   record. However, our sample size is large enough to begin unravelling Taumako bone

322   remodelling differences across the three anthropological age categories. The entire sample

323   followed an expected trend in secondary bone change with age, whereby both osteons and

324   vascular porosity increased through the lifespan in mature individuals [72, 73]. Further, all

325   the bone histology data appeared to peak at the middle-age category, which mirrors the

326   expectation based on modern bone health through the life-course paradigms. We

327   acknowledge such comparison cannot be exact given the broad age anthropological

328   categories, but the end of the young, and the start of the middle-age age category, overlaps

329   with the peak age for bone mass accrual in living humans [2]. When considering intra-

330   cortical osteon densities and canal-osteon ratios, it becomes apparent that Taumako females

331   maintain similar localised amounts of bone as males across different age categories. This

332   aligns with the same age-related observation in 1250–1450 AD Sudanese Kulubnarti, Nubia,

333   where no statistically significant changes in the geometric parameters of osteons were

334   observed [43]. Our data also match some of the findings reported by Burr et al. [62] for the

335   Pecos females who appeared to maintain good bone well into adulthood, and any age-related

336   reduction in bone quality was that of marrow cavity expansion in both males and females.

337   Generally, a smaller secondary osteon size has been previously noted to occur with age in

338   both males and females today [73], which applies to our results, and is similar to previous

339   reports for the Pecos males [62].

340

341   A preliminary and cautious comment about bone histology in our old males and females can

342   also be made. Although osteons were only measured in four well-preserved histology

343   samples, repressing four different individuals, all had densely remodelled Haversian bone.

344   There was no indication of early stages of osteoporosis, including cortical bone

345   trabecularisation or the presence of 'giant' coalescing pores [13]. Further, osteon density data

346   in the one old female matched osteon density data for the female middle-age category, and

347   were higher than the combined osteon density data in all three old male samples. We cannot

348   exclude the effect of osteon population density asymptote on the data in the old category,

349   whereby the evidence of pre-existing secondary osteons may have been erased by subsequent

350   generations of remodeled bone [74]. However, we can build a hypothesis, worth testing in

351 future bioarchaeological research, whether bone histology from old archaeological females
352 exhibits severe porosity (in the sense of trabecularisation, not just vascular counts) intra-
353 cortically [75]. This would help in validating to what extent, and at what age, past human
354 female long bone cortex develops osteoporosis in the fifth life decades or later. While most
355 anthropological methods of age estimation do not provide specific chronological ages, or
356 decades, some studies have recognised it might be possible to separate individuals aged 50+
357 years old into further age classes [76, 77]. Histological sampling in such instances could
358 contribute to this vein of research wherein older individuals could be gradually examined
359 decade by decade (similar to modern efforts, e.g. [75]). Although, a detailed contextual
360 information and burial/population background [78], along with permissions for destructive
361 sampling, would be needed.
362

363 Our study highlights the significance of combining gross anatomical and microscopic
364 approaches to understanding bone biology in archaeological contexts. Robb et al. [54]
365 reported some effect of age on metacarpal cortical bone indices, and femoral length, in the
366 Taumako sample without accessing microstructural indicators of cortical bone remodelling.
367 Our robusticity indices were calculated for femora instead of just reporting length, and
368 followed a robusticity methodological recommendation based on a published thorough
369 technical evaluation of different robusticity measures [55]. It will be important for future
370 bioarchaeological studies to combine macro- and microscopic technical approaches as limb
371 bone size and shape determined through ontogenetic modelling completes after the first two
372 life decades [79]. While modelling declines for the remainder of the lifespan, and re-activates
373 in extreme biomechanical situations, bone remodelling information can be only accessed
374 microscopically.
375

376   **REMARKS ON TEMPORAL AND SPATIAL BONE HISTOLOGY DATA**

377 We acknowledge that bone histology interpretations in archaeological settings need to be
378 conducted at a population level, but given our study presents the first osteon remodelling data
379 for the Pacific region, we can establish that the Taumako data fall into a global range of
380 secondary osteon parameters for archaeological humans [38, 43, 45, 62, 63]. Some examples
381 include: the Taumako male and female combined average osteon area (28,433 μm²) data are
382 similar to 27,303 μm² reported for medieval Canterbury, England [38, 45]; the male and
383 female combined area of Haversian canals in Taumako is 2,221 μm² which compares closely

384   to 2,100 μm² in medieval (1250–1450 AD) Sudanese Kulubnarti, Nubia [43], 2,336 μm² in

385   14th-19th centuries Pecos, New Mexico [62], and 2,334 μm² in medieval Canterbury, England

386   [38, 45]. Similarities can also be noted in raw osteon density data, whereby the Taumako data

387   of 13.64/mm² are close to 11.78/mm² in Sudanese Nubia [43]. We acknowledge the above

388   studies used slightly different region of interest (ROI) selection techniques, but all considered

389   femoral midshaft cortical bone. Future bone histology research on archaeological specimens

390   spanning other geographical regions will expand this range.

391

392   **LIMITATIONS**

393   We cannot exclude a series of confounding factors that have impacted our results and

394   interpretations. The estimates of age and sex for a portion of the sample at Taumako rely on

395   anthropological standards, as such they are probability scores. However, the aDNA validation

396   of the bulk of the sex estimates in this study overcame some of the uncertainty of gross

397   methods. Age assessments were validated as much as possible by ensuring that each

398   individual's histology profile generally matched its age status established from the gross

399   anatomical methods (e.g. thin sections were inspected for possible presence of primary bone

400   in samples from older adults). Unfortunately, we cannot overcome the inconsistencies in

401   sample size in each age and sex sub-group either, and do not have access to better preserved

402   bone histology. It must be said that some of the statistically insignificant results could simply

403   be a result of sampling given the specimens available to us, which is an issue for all

404   bioarchaeological studies. Finally, we only use two-dimensional methods of thin sectioning,

405   but a wider volumetric dataset providing three-dimensional perspectives on vascularity

406   connectedness, in combination with mineral density information, would provide a more in-

407   depth picture of bone building and remodelling capacities in the Taumako sample.

408

409   **CONCLUSIONS**

410   The Pacific islands are yet to be thoroughly studied for past human bone histological

411   variation. Our study forms the first, largest sample size based, report of archaeological human

412   intra-cortical secondary osteon, and cortical vascular porosity, data in this part of the world.

413   We found that archaeological females at Taumako show highly vascularised femoral

414   midshaft bone, but also have localised areas of intra-cortical bone that remodels similarly to

415   that of males. This finding mirrors bone remodelling data from other archaeological sites

416   from across North America, Europe, and Africa, but does not conform entirely to our modern

understanding of bone loss through the life-course. These new data fall in the range of bone histology archaeological variability reported globally, extending currently available bone histology data by this site from the Pacific Islands. The lower vascular porosity in males might reflect their higher frailty in the cultural and environmental context of Taumako, and the balanced remodelling indicators between the sexes could be a result of socially stratified dietary practices. Ongoing efforts examining bone histology in Asia-Pacific will further our understanding of ancient human bone remodelling capacities in this region, contributing to modern efforts investigating the conditions under which human experience significant bone loss.

MATERIALS AND METHODS

Taumako is one of the remote Duff Islands, which lie northeast of Santa Cruz Islands in the far southeast Solomon Islands [15] (Figure 1). While the island is located within the Melanesian geographical boundary, Taumako is known as a 'Polynesian Outlier' representing a probable 'blow-back' migration of populations from Polynesia around the mid-second millennium AD [15, 81, 81]. The modern inhabitants of Taumako speak a Polynesian language, but as a result of admixture with established populations, share similar cultural traditions to nearby Melanesian islands in the Duff and Santa Cruz groups [82].

The Namu burial mound, an archaeological site dated to ca. 440-150 BP [20], yielded a significant number of human remains and associated grave goods that have been since examined to reconstruct the lives of the past inhabitants of Taumako. This has included social status stratification [15, 17] reflected in dietary and child feeding practices reconstructed from bone and tooth stable isotope data [16, 17, 26, 83]; abnormalities of the alveolar bone suggesting possible experiences of periodontitis [84]; evidence for interpersonal violence and warfare inferred from skeletal patterns of trauma [85]; a high prevalence of yaws (*Treponema pertenue*) [24]; and, more recently, gender specific migration patterns from neighbouring islands [20]. The site is known for archaeological evidence of using shell money and ornamentation practices that include a *tavi* - a neck ornament thought to represent high status (see [15]). Another study also analysed Taumako femur length and metacarpal and femur cortical indices and noted a lack of distinct bone functional adaptation in remote Pacific Island environments [54].

450   With permissions from, and in collaboration with, the Solomon Islands National Museum, n

451   = 69 Taumako adults were sampled in the present study. There were 19 left and 50 right

452   femora. Both sides were pooled due to no statistically significant bilateral differences in the

453   recorded data (Supplementary Information Tables 1, 2). Following standard methods

454   recommended by Buikstra and Ubelaker [57], and Brickley and McKinley [58], each

455   individual was thoroughly examined for skeletal markers of sex, and those that change with

456   age, to arrive at morphologically informed biological sex and age-at-death (we use 'age' in

457   the main article) estimates. The age categories follow these standard recommendations

458   whereby individuals are assigned into 'young' (20–35 years old), 'middle-aged' (36–50 years

459   old) and old (50+ years old) age-at-death classes. As is good practice in bioarchaeology, for

460   each individual, as many techniques of examination were applied as possible to increase the

461   accuracy of the estimates. These methods involve a gross anatomical examination of the

462   following: dental wear of permanent teeth with higher degrees of wear progressing with age;

463   obliteration degree of cranial sutures which progressively close with age; texture and general

464   morphology changes of the pelvic auricular surface and the pubic symphysis, which

465   disintegrate with age. Each skeletal technique gives an independent age range, which are then

466   compiled into common ranges that can be placed into the major age-at-death classes. We

467   have no way of corroborating the anthropological estimates, which are necessarily broad,

468   with actual chronological age of these individuals, which is unknown.

469

470   The biological sex estimation was based upon examining the skull and pelvic anatomical

471   landmarks which are known to be sexually dimorphic. A non-exhaustive list of these features

472   includes: the robusticity level of the mastoid process; the nuchal crest of the occipital bone;

473   the shape of the eye orbits and the thickness of the orbital roof; the prominence of the

474   glabella; and the mental eminence of the mandible; the angle of the pelvic sciatic notch; the

475   presence or absence of the pelvic ventral arc, subpubic concavity, and a medial ridge in the

476   pubis region.

477

478   Skeletal morphology is more robust in the male skeletal remains, though we acknowledge

479   this is a generalisation. Thus, unlike with our age-at-death estimates, with permission from

480   the Solomon Islands Museum, we were able to validate the sex estimates through aDNA

481   obtained from genome-wide data that had been produced for a subset of samples investigated

482   histologically. Individuals were sampled for DNA by drilling the petrous part of the temporal

483 bone [86] (see dataset [87]). DNA was extracted from the sampled powder and prepared for

484 next-generation sequencing by producing a double-stranded DNA library following

485 established protocols [88, 89, 90]. Deaminated cytosines were enzymatically partially

486 removed and retained only in the terminal positions as described in [91]. All libraries were

487 directly shotgun sequenced on an Illumina HiSeq 4000 platform ($1 \times 75 + 8 + 8$ cycles). The

488 sequenced reads were mapped to the human genome reference hg19 using EAGER [92]. The

489 retained damage was excluded from the analysis by masking the two terminal positions of

490 each read [93]. The genetic sex was inferred using two independent methods:

491

492 1) The number of reads covering each position was counted across a total of around 1.24

493   million genome-wide SNP positions [94, 95, 96] and subsequently averaged for each

494   sex chromosome and all autosomal ones. The Y- and the X- chromosome average

495   coverages were normalized by the average autosomal coverage and compared to

496   determine the sex assignment [97].

497 2) An approach specifically designed for low-covered shotgun genomes in which the

498   ratio between the average coverage across the entire X-chromosome and the coverage

499   averaged across the autosomes was calculated as in [98] (see Supplementary

500   Information for extended aDNA methods). This was possible for n = 48 individuals.

501   There was an 88% success rate (42/48) in corroborating the macroscopic and aDNA

502   sex results, with only six individuals misclassified by the gross methodologies (see

503   Supplementary Information Table 3). Therefore, the presented sex classification can

504   be treated as fairly reliable. We acknowledge we do not attempt to classify these as

505   'gender', but treat them as a biological entity in relation to bone metabolic processes.

506   As a result, this study comprised 34 young adults, 13 middle-aged adults, 22 old

507   adults, and 36 females and 33 males. Further sub-division by age-at-death within each

508   sex group can be seen in the dataset [87].

509 Prior to histological analyses we recorded a series of femur morphometric measurements to

510 characterise the size of each femoral midshaft and calculate femoral robusticity indices where

511 possible [55, 60]. Three variables were included: midshaft circumference (Circ) in mm,

512 posterior cortical width (Ct.W) in mm, and femur maximum length in cm. These were

513 measured using standard osteological laboratory equipment composed of an osteometric

514 board, digital calipers, and a soft measuring tape. Two robusticity indices were computed

515 using the Stock and Shaw [55] recommendation and following prior methods combining

516   femoral bone histology and robusticity measures [45]: femoral robusticity index based on
517   Circ where the circumference values are divided by femoral length, and a femoral robusticity
518   index based on Ct.W where cortical width values are divided by femoral length and
519   multiplied by 100. The latter included multiplication by 100 to increase decimals in the
520   resulting robusticity index values for the ease of our statistical analysis. Only 23 femora were
521   of a suitable preservation for measuring the maximum length, and so only these were used in
522   the robusticity index calculations.

523

524   Next, posterior cortical bone samples from the midshaft of each femur were extracted using a
525   Dremel tool with a rotary blade, resulting in approximately 1cm thick cortical quadrants (see
526   [45]). The posterior femur is of interest to our study because it overlaps the *linea aspera*, a
527   rich leg muscle site insertion anatomical landmark. Bone remodelling detected there should
528   capture stimulation resulting from lifestyle [99, 100], which will strengthen our analyses of
529   age and sex. Our minimal invasive approach ensured the femora remained as intact as
530   possible, limiting the amount of archaeological bone being taken for the histological analysis
531   [101]. Standard histological methods relevant to archaeological human remains were then
532   followed to produce ~100 μm thin sections [34]. Each sample was embedded in Buehler
533   epoxy resin, cut using a Kemet MICRACUT precision cutter equipped with a diamond blade,
534   glued to a microscope slide, further reduced, ground, and polished to obtain a clear view of
535   bone histology. The thin sections were examined using an Olympus BX53 microscope with a
536   DP74 camera using transmitted and linearly polarised light at a magnification of 10x (100x
537   total magnification).

538

539   Once histology slides were prepared, it became apparent that not all microstructures could be
540   measured in all sections. Well preserved ROIs where cement lines of secondary osteons were
541   easily identifiable were the case for only 21 individuals, but 68 individuals had consistently
542   and suitably preserved Haversian canals. A diagenetically obscured band that ran along the
543   outer posterior and endosteal layers of bone samples was also observed in the thin sections.
544   However, the intra-cortical regions of bone were of an almost pristine preservation, which
545   allowed us to focus on intra-cortical remodelling activity away from the immediately sub-
546   periosteal and sub-endosteal regions of cortical bone. As such, we designed the ROI selection
547   procedure so that data can be collected from the mid-portion of each sample by scanning a
548   full cortical strip down the midline and then capturing three ROIs within its centre (Figure 2).

549 The examination of cortical strips as ROIs, and intra-cortical bone regions generally, were

550 successful in prior archaeological studies [44, 102].

551

552 We used the Olympus cellSens software ("Standard" version 2018, https://www.olympus-

553 lifescience.com/en/software/cellsens/), which allows to automatically stitch images in live

554 scanning mode. This function was used used to record each ROI 'strip'. A thin section was

555 placed on the microscope stage so that the mid-point of the periosteal border was in the field

556 of view. The stage was then slowly moved forward (away from the observer) until the endosteal

557 end of the border was reached. The area of the ROI strips ranged from 6.76 mm^2 to 25.84 mm^2

558 in our sample given variation in cortical wall thickness (mean = 14 mm^2, standard deviation =

559 3.67 mm^2). From within the strip, the first ROI was located at the mid-point (by dividing the

560 length of the entire strip by two), and then one ROI was taken either side of this midpoint,

561 ensuring no overlap in histology shown in the field of view (Figure 2). Using FIJI/ImageJ tools

562 that included the "Multi-Point Count" and "Polygon" selections, three histomorphometric

563 variables indicative of cortical bone remodelling events were measured (we use bone

564 histomorphometry nomenclature recommended by Dempster et al. [103] Figure 2):

565

566 - **Vascular porosity** (V.Po) per mm^2 (e.g. [13, 62, 104, 105]): total number of intact
567   Haversian and primary canals across a full strip ROI of bone measured from the
568   posterior to the endosteal borders of the section, and divided by the strip area in mm^2.
569   Volkmann's canals were excluded because they were rarely visible in the sample.
570   Because we worked with archaeological specimens and 2D histology sections, true
571   vascular porosity, including other minute capillaries is not possible to obtain. In
572   instances where cement lines of osteons were not visible, we cannot be entirely
573   confident that a counted canal derives from a secondary osteon structure. As such, we
574   use V.Po to represent all major vascular canals seen in the ROI strip.

575 - **Osteon population density** (OPD) per mm^2 (e.g. 43, 45): sum of intact osteon and
576   fragmentary osteon numbers counted from three intra-cortical ROIs of 2.05 mm^2 area
577   each (totalling 6.15 mm^2). Each sum was divided by the ROI area in mm^2.

578 - **Haversian canal:Osteon area ratio** (H.Ar/On.Ar), measured in μm² separately, and
579   then converted to unitless (dimensionless variable (DV)) ratio values (e.g. [45, 56,
580   60]): H.Ar is the average area (total area/total number of measured canals) of intact
581   Haversian canals measured from three intra-cortical ROIs of 2.05 mm^2 area each
582   (totalling 6.15 mm^2); On.Ar is the secondary osteon area in μm² created from average

583   area (total area/total number of measured secondary osteons) of intact secondary

584   osteons with complete cement lines measured from three intra-cortical ROIs of 2.05

585   mm^2 area each (totalling 6.15 mm^2). Secondary osteons cut off by an image border

586   were excluded. The average values of H.Ar are then divided by the average values of

587   On.Ar and multiplied by 100 to indicate percentage of canal to osteon area.

588 Recommended standards for reporting of bone histomorphometric data stipulate a minimum

589 of 25 osteons examined per thin section [40]. Our study meets those standards by examining

590 a minimum of 47 and maximum of 126 secondary osteons across the samples for the

591 purposes of osteon density calculations, and minimum 25 and maximum 50 for the purpose

592 of ratio calculations from area measurements of osteon units. The V.Po and OPD data are

593 used in our study as products of bone remodelling events that indicate the amount of bone

594 produced and remodeled per mm^2 intra-cortically [45]. The area of Haversian canals and

595 secondary osteons can be used as indicators of the stage of a BMU travelling through the

596 cortex [36]. Larger areas of osteons and canals can be associated with longer periods of BMU

597 activity, and smaller areas would indicate a shorter-term BMU activity, particularly if it is

598 strain-suppressed [38, 106].

599

600 Prior to addressing the main questions of our study, we ran non-parametric Spearman's *Rho*

601 tests (due to sample size smaller than 30 in at least one sub-group that was being included in

602 the correlations) correlating all the histology variables to check whether porosities, densities,

603 and area measures increased or decreased in values when considered alongside each other.

604 This step was necessary as we have different histology data from two different types of ROIs

605 (the 'strip' and three localised ROIs within), so we wanted to check that each variable can be

606 treated independently in our interpretation. Statistically significant relationships, and those of

607 *Rho* > 0.35 [107], were taken to indicate that the variables reflected expected relationships

608 such as allometry between osteon and canal area, and the density variables [60]. The

609 histology correlations returned three statistically significant and strong relationships (Figure

610 4; Supplementary Information Table 4) for the area of osteons and their Haversian canals

611 (positive correlation), osteon area and population density (negative correlation), and vascular

612 porosity and osteon population density (positive correlation). The area of osteons increased as

613 the area of canals increased, higher osteon densities were associated with smaller osteons

614 (which is expected for a strained posterior femur), and higher vascular porosities

615 corresponded to higher osteon densities. This information means that despite collecting

different histology data from different ROIs, all related to one another statistically allowing us to interpret them all in the comparisons with age and sex.

Next, the V.Po and OPD variables were adjusted by the previously measured midshaft variables and calculated RIs to account for a possible isometric relationship between femur size and the underlying histological structures [61, 61]. It is possible that larger femora could simply show higher values of canals and osteons as a result of inherent size variation across the sample. This was also important as previous research indicated that sexually dimorphic bones may still build bone tissue of similar quality [108].

The H.Ar/On.Ar ratio variable did not require adjustments as it is in itself already a quantitative relation between two histology measures of size. The V.Po variable was adjusted by raw Circ and Ct.W (creating V.Po/Circ, and V.Po/Ct.W), whereas OPD was adjusted by robusticity index (Circ) and robusticity index (Ct.W) where the femoral maximum length was available for robusticity index calculations.

A brief descriptive analysis summarising data using mean, minimum, maximum, and standard deviation (SD) values was conducted in first instance. The quantitative variables in n > 30 (Circ, Ct.W, V.Po, V.Po/Ct.W, V.Po/Circ) were tested for normality using the Kolmogorov-Smirnov test. Parametric tests were then selected for normally distributed variables (Circ, Ct.W, V.Po, V.Po/Circ), and non-parametric tests were applied to V.Po/Ct.W where data were not normally distributed. For data in sub-groups of n < 30, non-parametric inferential tests were selected without normality tests given the sample size. As a result, Mann-Whitney U tests or t-tests were applied when comparing bone macro- and microstructure between the sexes. When comparing the three age-at-death groups, we used a non-parametric Kruskal-Wallis test with a post-hoc pairwise comparison. For the gross femoral analyses we report significant results only, whereas for the histology analyses we show all results because they are interpreted to answer our research questions. We did not run statistical analyses on the OPD data, and age-at-death and sex sub-divisions due to inadequate sample size in the sub-groups.

REFERENCES

1. Gordon, C.M. *et al.* 2017. The determinants of peak bone mass. *J. Paediatr.* **180**, 261-269 (2017).

2. Heaney, R.P. *et al.* Peak bone mass. *Osteoporos. Int.* **11,** 985 (2000).

3. Seeman, E. Reduced bone density in women with fractures: contribution of low peak bone density and rapid bone loss. *Osteoporos. Int.* **4**, S15-S25 (1994).

4. Kanis, J.A. Estrogens, the menopause, and osteoporosis. *Bone* **19,** 185S-190S (1996).

5. Lindsay, R. The menopause and osteoporosis. *Obstet. Gynecol.* **87,** 16S-19S (1996).

6. Riggs, B.L. The mechanisms of estrogen regulation of bone resorption. *J. Clin. Investig.* **106,**1203-1204 (2000).

7. Robling, A.G., Castillo, A.B., Turner, C.H. Biomechanical and molecular regulation of bone remodeling. *Ann. Rev. Biomed. Eng.* **8**, 455-498 (2006).

8. Agarwal, S.C. Bone morphologies and histories: Life course approaches in bioarchaeology. *Am. J. Phys. Anthropol.* **159,** 130-149 (2016).

9. Agarwal, S.C., Grynpas, M.D. Bone quantity and quality in past populations. *Anat. Rec.* **246**, 423-432 (1996).

10. Agarwal, S.C., Stout, S.D. *Bone Loss and Osteoporosis: An Anthropological Perspective* (Springer, 2003).

11. Miszkiewicz, J.J., Cooke, K.M. Socio-economic determinants of bone health from past to present. *Clinic. Rev. Bone. Miner. Metab.* **17**, 109-122 (2019).

12. Miszkiewicz, J.J., Brennan-Olsen, S., Riancho, J.A. *Bone Health: A Reflection of The Social Mosaic.* (Springer, 2019).

13. Miszkiewicz, J.J. *et al.* Bone loss markers in the earliest Pacific Islanders. *Sci. Rep.* **11,** 1-6 (2021).

14. Miszkiewicz, J.J., Matisoo-Smith, E.A., Weisler, M.I. Behavior and intra-skeletal remodeling in an adult male from 1720 BP Ebon Atoll, Marshall Islands, eastern Micronesia. *J. Isl. Coast. Archaeol.* **17**, 445-459 (2022).

15. Leach, F., Davidson, J. The Archaeology on Taumako: A Polynesian Outlier in the Eastern Solomon Islands. *Dunedin: New Zealand Journal of Archaeology* (2008).

16. Kinaston, R.L., Buckley, H.R. Isotopic insights into diet and health at the site of Namu, Taumako Island, Southeast Solomon Islands. *Archaeol. Anthropol. Sci.* **9,** 1405-1420 (2017).

699   17. Kinaston, R.L., Buckley, H.R., Gray, A. Diet and social status on Taumako, a
700   Polynesian outlier in the Southeastern Solomon Islands. *Am. J. Phys. Anthropol.* **151,**
701   589-603 (2013).
702
703   18. Gosling, A.L., Matisoo-Smith, E.A. The evolutionary history and human settlement of
704   Australia and the Pacific. *Curr. Opin. Genet. Dev.* **53,** 53-59 (2018).
705
706   19. Davidson, J.M. Polynesian outliers and the problem of cultural replacement in small
707   populations. In: Green RC, Kelly M, editors. *Studies in Oceanic Culture History*
708   *Volume I, Pacific Anthropological Records 11*. Honolulu: Bernice P. Bishop Museum,
709   p. 61–72 (1970).
710
711   20. Kramer, R.T. *et al*. Strontium (87Sr/86Sr) isotope analysis of the Namu skeletal
712   assemblage: A study of past human migration on Taumako, a Polynesian Outlier in
713   the eastern Solomon Islands. *Am. J. Phys. Anthropol.* **174**, 479-499 (2021).
714
715   21. Gosling, A.L., Buckley, H.R., Matisoo-Smith, E., Merriman, T.R. Pacific populations,
716   metabolic disease and 'Just-So Stories': A critique of the 'Thrifty Genotype'
717   hypothesis in Oceania. *Ann. Human. Genet.* **79,** 470-480 (2015).
718
719   22. Tsuchiya, C., Tagini, S., Cafa, D., Nakazawa, M. Socio-environmental and behavioral
720   risk factors associated with obesity in the capital (Honiara), the Solomon Islands;
721   case-control study. *Obes. Med.* **7,** 34-42 (2017).
722
723   23. Buckley, H.R. *Health and Disease in the Prehistoric Pacific Islands*. Oxford, UK:
724   British Archaeological Reports International Series 2792. (British Archaeological
725   Reports Ltd, 2016).
726
727   24. Buckley, H.R., Tayles, N. Skeletal pathology in a prehistoric Pacific Island sample:
728   issues in lesion recording, quantification, and interpretation. *Am. J. Phys. Anthropol.*
729   **122,** 303-324 (2003).
730
731   25. Cooke, K. M. *et al.* Paleohistopathology of treponemal disease in human bone from
732   Taumako, Solomon Islands (700-300ybp). *Am. J. Biol. Anthropol.* **177**, 36 (2022).
733
734   26. Stantis, C., Buckley, H. R., Commendador, A., Dudgeon, J. V. Expanding on
735   incremental dentin methodology to investigate childhood and infant feeding practices
736   on Taumako (southeast Solomon Islands). *J. Archaeol. Sci.* **126**, 105294 (2021).
737
738   27. Ebeling, P.R. *et al.* Secondary prevention of fragility fractures in Asia Pacific: an
739   educational initiative. *Osteoporos. Int.* **31,** 805-26 (2020).
740
741   28. Khosla, S., Farr, J.N., Tchkonia, T., Kirkland, J.L. The role of cellular senescence in
742   ageing and endocrine disease. *Nat. Rev. Endocrinol.* **16,** 263-75 (2020).
743
744   29. Medina-Gomez, C. *et al*. Life-course genome-wide association study meta-analysis of
745   total body BMD and assessment of age-specific effects. *Am. J. Hum. Genet.* **102,** 88-
746   102 (2018).
747

748   30. Gourlay, M.L., Hammett-Stabler, C.A., Renner, J.B., Rubin, J.E. Associations
749   between body composition, hormonal and lifestyle factors, bone turnover, and BMD.
750   *J. Bone. Metab.* **21,** 61-68 (2014).
751
752   31. Bianchi, M.L., Sawyer, A.J., Bachrach, L.K. Rationale for bone health assessment in
753   childhood and adolescence. In: Fung E, Bachrach L, Sawyer A, editors. *Bone Health*
754   *Assessment in Paediatr*ics. Cham: Springer. p 1-21 (2016).
755
756   32. Link, T.M. Metabolic bone disease. In: Cassar-Pullicino VN, Davies AM, editors.
757   *Measurements in Musculoskeletal Radiology*. Berlin: Springer, p 785-807 (2020).
758
759   33. Agarwal, S. C. What is normal bone health? A bioarchaeological perspective on
760   meaningful measures and interpretations of bone strength, loss, and aging. *Am. J.*
761   *Hum. Biol.* **33**, e23647 (2021).
762
763   34. Miszkiewicz, J.J., Mahoney, P. Human bone and dental histology in an archaeological
764   context. In: Errickson D, Thompson T, editors. *Human Remains: Another Dimension.*
765   *The Application of Imaging to the Study of Human Remains*. Cambridge: Elsevier
766   Academic Press, p 29-43 (2017).
767
768   35. Crowder, C., Stout, S.D. *Bone Histology: An Anthropological Perspective*. (CRC
769   Press, 2011).
770
771   36. Lassen, N.E. *et al*. Coupling of bone resorption and formation in real time: new
772   knowledge gained from human Haversian BMUs. *J. Bone. Miner. Res.* **32**, 1395-405
773   (2017).
774
775   37. Britz, H.M., Thomas, C.D.L., Clement, J.G., Cooper, D.M. The relation of femoral
776   osteon geometry to age, sex, height and weight. *Bone* **45,** 77-83 (2009).
777
778   38. Miszkiewicz, J.J. Investigating histomorphometric relationships at the human femoral
779   midshaft in a biomechanical context. *J. Bone Miner. Metab.* **34,** 179-192 (2016).
780
781   39. van Oers, R.F., Ruimerman, R., van Rietbergen, B., Hilbers, P.A., Huiskes, R.
782   Relating osteon diameter to strain. *Bone* **43**, 476-482 (2008).
783
784   40. Stout, S.D., Crowder, C. Bone remodeling, histomorphology, and histomorphometry.
785   In: Crowder C, Stout SD, editors. Bone Histology: An Anthropological Perspective.
786   Boca Raton: CRC Press, p 1– 21 (2011).
787
788   41. Cardoso, L., Fritton, S.P., Gailani, G., Benalla, M., Cowin, S.C. Advances in
789   assessment of bone porosity, permeability and interstitial fluid flow. *J. Biomech.* **46**,
790   253-65 (2013).
791
792   42. Cooper, D. M. L., Kawalilak, C. E., Harrison, K., Johnston, B. D., Johnston, J. D.
793   Cortical bone porosity: what is it, why is it important, and how can we detect it?.
794   *Curr. Osteoporos. Rep*. **14**, 187-198 (2016).
795
796   43. Mulhern, D.M., Van Gerven, D.P. Patterns of femoral bone remodeling dynamics in a
797   medieval Nubian population. *Am. J. Phys. Anthropol.* **104,** 133-146 (1997).

798   44. Robling, A.G., Stout, S.D. Histomorphology, geometry, and mechanical loading in
799   past populations. In: Agarwal SC, Stout SD, editors. *Bone Loss and Osteoporosis: An*
800   *Anthropological Perspective*. Boston: Springer, p 189-205 (2003).

801

802   45. Miszkiewicz, J.J., Mahoney, P. Ancient human bone microstructure in medieval
803   England: comparisons between two socio-economic groups. *Anat. Rec.* **299**, 42-59
804   (2016).

805

806   46. Pfeiffer, S. Variability in osteon size in recent human populations. *Am. J. Phys.*
807   *Anthropol.* **106**, 219-227 (1998).

808

809   47. Pfeiffer, S., Crowder, C., Harrington, L., Brown, M. Secondary osteon and Haversian
810   canal dimensions as behavioral indicators. *Am. J. Phys. Anthropol.* **131**, 460-468
811   (2006).

812

813   48. Streeter, M., Stout, S., Trinkaus, E., Burr, D. Bone remodeling rates in Pleistocene
814   humans are not slower than the rates observed in modern populations: A
815   reexamination of Abbott et al.(1996). *Am. J. Phys. Anthropol.* **141**, 315-318 (2010).

816

817   49. Abbott, S., Trinkaus, E., Burr, D.B. Dynamic bone remodeling in later Pleistocene
818   fossil hominids. *Am. J. Phys. Anthropol.* **99,** 585-601 (1996).

819

820   50. Buckley, H. Epidemiology of gout: Perspectives from the past. *Curr. Rheumatol. Rev.*
821   **7**, 106-113 (2011).

822

823   51. Buckley, H.R., Oxenham, M. Bioarchaeology in the Pacific Islands: a temporal and
824   geographical examination of nutritional and infectious disease. In: Oxenham M,
825   Buckley H, editors. *The Routledge Handbook of Bioarchaeology in Southeast Asia*
826   *and the Pacific Islands*. London: Routledge, p. 363-388 (2016).

827

828   52. Foster A, et al. 2018. Possible diffuse idiopathic skeletal hyperostosis (DISH) in a
829   3000-year-old Pacific Island skeletal assemblage. *J Archaeol Sci: Rep* **18**: 408-419.

830

831   53. Buckley, H.R. *et al.* Scurvy in a tropical paradise? Evaluating the possibility of infant
832   and adult vitamin C deficiency in the Lapita skeletal sample of Teouma, Vanuatu,
833   Pacific islands. *Int. J. Palaeopathol.* **5**, 72-85 (2014).

834

835   54. Robb, K.F., Buckley, H.R., Spriggs, M., Bedford, S. Cortical index of three
836   prehistoric human Pacific Island samples. *Int. J. Osteoarchaeol.* **22**, 284-293 (2012).

837

838   55. Stock. J.T., Shaw, C.N. Which measures of diaphyseal robusticity are robust? A
839   comparison of external methods of quantifying the strength of long bone diaphyses to
840   cross-sectional geometric properties. *Am. J. Phys. Anthropol.* **134,** 412-423 (2007).

841

842   56. Cooke, K. M., Mahoney, P., & Miszkiewicz, J. J. (2022). Secondary osteon variants
843   and remodeling in human bone. *Anat. Rec.* **305**, 1299-1315.

844

845   57. Buikstra, J.E., Ubelaker, D.H. *Standards for Data Collection from Human Skeletal*
846   *Remains*. (Colorado Historical Society, 1994).

847

848   58. Brickley, M., & McKinley, J. (2004). Guidance to standards for recording human
849   skeletal remains. IFA Technical Paper 7. IFA.
850

851   59. DuBois, L. Z., Shattuck-Heidorn, H. Challenging the binary: Gender/sex and the bio-
852   logics of normalcy. *Am. J. Hum. Biol*. **33**, e23623 (2021).
853

854   60. Miszkiewicz, J.J., Mahoney, P. Histomorphometry and cortical robusticity of the adult
855   human femur. *J. Bone. Miner. Metab.* **37**, 90-104 (2019).
856

857   61. Goldman, H. M., Hampson, N. A., Guth, J. J., Lin, D., Jepsen, K. J. Intracortical
858   remodeling parameters are associated with measures of bone robustness. *Anat.*
859   *Rec.* **297**,1817-1828 (2014).
860

861   62. Burr, D.B., Ruff, C.B., Thompson, D.D. Patterns of skeletal histologic change through
862   time: comparison of an archaic Native American population with modern populations.
863   *Anat. Rec.* **226**, 307-313 (1990).
864

865   63. Thompson, D.D., Salter, E.M., Laughlin, W.S. Bone core analysis of Baffin Island
866   skeletons. *Arc. Anthropol.* **18**, 87-96 (1981).
867

868   64. Miszkiewicz, J.J., Stewart, T.J., Deter, C.A., Fahy, G.E., Mahoney, P. Skeletal Health
869   in Medieval Societies: Insights from Ancient Bone Collagen Stable Isotopes and
870   Dental Histology. In: Miszkiewicz JJ, Brennan-Olsen S, Riancho JA, editors. Bone
871   Health: A Reflection of the Social Mosaic. Singapore: Springer Nature, p 17-34
872   (2019).
873

874   65. Bachrach, L.K. Skeletal Development in Childhood and Adolescence. Primer on the
875   Metabolic Bone Diseases and Disorders of Bone Metabolism. Hoboken: Wiley, p. 74-
876   79 (2009).
877

878   66. Klein, S.L. The effects of hormones on sex differences in infection: from genes to
879   behavior. *Neurosci. Biobehav. Rev.* **24**, 627-638 (2000).
880

881   67. Stinson, S. Sex differences in environmental sensitivity during growth and
882   development. *Am. J. Phys. Anthropol.* **28**, 123-147 (1985).
883

884   68. Furusawa, T., Aswani, S. Well-nourished women in a Solomon Islands society with a
885   biased sex ratio. *Pacific Health Dialog.* **17**, 77-81 (2011).
886

887   69. Kinaston, R. *Prehistoric Diet and Health in the Western Pacific Islands*. PhD Thesis,
888   University of Otago, Dunedin, New Zealand (2010).
889

890   70. Ross, R.D., Sumner, D.R. Bone matrix maturation in a rat model of intra-cortical bone
891   remodeling. *Calcif. Tiss. Int.* **101**, 193-203 (2017).
892

893   71. Ruth, E.B. Bone studies. II. An experimental study of the Haversian-type vascular
894   channels. *Am. J. Anat.* **93**, 429-455 (1953).
895

896   72. Wang, X., Ni, Q. Determination of cortical bone porosity and pore size distribution
897   using a low field pulsed NMR approach. *J. Orthop. Res.* **21**, 312-319 (2003).

73. Currey, J.D. Some effects of ageing in human Haversian systems. *J. Anat.* **98,** 69 (1964).

74. Frost, H.M. Secondary osteon population densities: an algorithm for estimating the missing osteons. *Am. J. Phys. Anthropol.* **30**, 239-254 (1987).

75. Zebaze. R.M. *et al.* Intracortical remodelling and porosity in the distal radius and post-mortem femurs of women: a cross-sectional study. *Lancet* **375**, 1729-36 (2010).

76. Cave, C., Oxenham, M. Identification of the archaeological 'invisible elderly': an approach illustrated with an Anglo-Saxon example. *Int. J. Osteoarchaeol.* **26**, 163-175 (2016).

77. McFadden, C., Cave, C. M., Oxenham, M. F. Ageing the elderly: A new approach to the estimation of the age-at-death distribution from skeletal remains. *Int. J. Osteoarchaeol.* **29**, 1072-1078 (2019).

78. Gowland, R. L. Elder abuse: evaluating the potentials and problems of diagnosis in the archaeological record. *Int. J. Osteoarchaeol.* **26**, 514-523 (2016).

79. Pearson, O.M., Lieberman, D.E. The aging of Wolff's "law": ontogeny and responses to mechanical loading in cortical bone. *Am. J. Phys. Anthropol.* **125**, 63-99 (2004).

80. Davidson, J. Cultural replacement on small islands: new evidence from polynesian outliers. *Mankind* **9**, 273-77 (1974).

81. Kirch, P.V. The Polynesian outliers: continuity, change, and replacement. *J. Pac. Hist.* **19**, 224-38 (1984).

82. Leach, F., Davidson, J., Davenport, W. Social organization notes on the northern Santa Cruz Islands: the Duff Islands (Taumako). *Baessler-Archiv. Neue. Folge.* **16**, 137-205 (1968).

83. Leach, H. Did East Polynesians have a concept of luxury foods?. *World Archaeol.* **34**, 442-457 (2003).

84. Fyfe, D.M., Chandler, N.P., Wilson, N.H.F. Alveolar bone status of some pre-seventeenth century inhabitants of Taumako, Solomon Islands. *Int. J. Osteoarchaeol.* **3**, 29-35 (1993).

85. Scott, R.M., Buckley, H.R. Biocultural interpretations of trauma in two prehistoric Pacific Island populations from Papua New Guinea and the Solomon Islands. *Am. J. Phys. Anthropol.* **142**, 509-518 (2010).

86. Pinhasi, R. D. *et al.* Optimal ancient DNA yields from the inner ear part of the human petrous bone. *PloS one* **10**, e0129102 (2015).

946   87. Miszkiewicz, J.J. *et al.* Data for Taumako sample: femur histology, femur
947   morphometry, genetic sex. Figshare dataset:
948   https://doi.org/10.6084/m9.figshare.16815295 (2022)
949

950   88. Dabney, J. *et al.* Complete mitochondrial genome sequence of a Middle Pleistocene
951   cave bear reconstructed from ultrashort DNA fragments. *Proc. Natl. Acad. Sci.*
952   *U.S.A.* **110**, 15758–15763 (2013).
953

954   89. Meyer, M., Kircher, M. Illumina sequencing library preparation for highly
955   multiplexed target capture and sequencing. *Cold Spring Harb. Protoc.* **2010**,
956   pdb.prot5448 (2010).
957

958   90. Kircher, M., Sawyer, S., Meyer, M. Double indexing overcomes inaccuracies in
959   multiplex sequencing on the Illumina platform. *Nucleic Acids Res.* **40**, e3 (2012).
960

961   91. Rohland, N., Harney, E., Mallick, S., Nordenfelt, S., Reich, D. Partial uracil–DNA–
962   glycosylase treatment for screening of ancient DNA. *Philos. Trans. R. Soc. Lond. B*
963   *Biol. Sci.* **370**, 20130624 (2015).
964

965   92. Peltzer, A. *et al.* EAGER: Efficient ancient genome reconstruction. *Genome Biol.* **17**,
966   60 (2016).
967

968   93. Jun, G., Wing, M. K., Abecasis, G. R., Kang, H. M. An efficient and scalable analysis
969   framework for variant extraction and refinement from population-scale DNA
970   sequence data. *Genome Res.* **25**, 918-925 (2015).
971

972   94. Fu, Q. *et al.* DNA analysis of an early modern human from Tianyuan Cave,
973   China. *Proc. Natl. Acad. Sci. U.S.A.* **110**, 2223–2227 (2013).
974

975   95. Haak, W. *et al.* Massive migration from the steppe was a source for Indo-European
976   languages in Europe. *Nature* **522**, 207–211 (2015).
977

978   96. Mathieson, I. *et al.* Genome-wide patterns of selection in 230 ancient
979   Eurasians. *Nature* **528**, 499–503 (2015).
980

981   97. Fu, Q., *et al.* The genetic history of ice age Europe. *Nature* **534**, 200-205 (2016).
982

983   98. Mittnik, A., Wang, C.C., Svoboda, J., Krause, J. A molecular approach to the sexing
984   of the triple burial at the Upper Paleolithic Site of Dolní Věstonice. *PloS one*, **11**,
985   p.e0163019. (2016).
986

987   99. Bell, K.L. *et al.* Super-osteons (remodeling clusters) in the cortex of the femoral shaft:
988   Influence of age and gender. *Anat. Rec.* **264**, 378-86 (2001).
989

990   100.   Chan, A.H., Crowder, C.M., Rogers, T.L. Variation in cortical bone histology
991   within the human femur and its impact on estimating age at death. *Am. J. Phys.*
992   *Anthropol.* **132,** 80-8 (2007).
993

101. Mays, S., Elders, J., Humphrey, L., White, W., Marshall, P. *Science and the dead: a guideline for the destructive sampling of archaeological human remains for scientific analysis.* English Heritage Publishing with the Advisory Panel on the Archaeology of Burials in England (2013).

102. Richman, E.A., Ortner, D.J., Schulter-Ellis, F.P. Differences in intracortical bone remodeling in three aboriginal American populations: possible dietary factors. *Calcif. Tiss. Int.* **28**, 209-214 (1979).

103. Dempster, D.W. *et al*. Standardized nomenclature, symbols, and units for bone histomorphometry: a 2012 update of the report of the ASBMR Histomorphometry Nomenclature Committee. *J. Bone Min. Res.* **28**, 2-17 (2013).

104. Ciani, C., Doty, S.B., Fritton, S.P. An effective histological staining process to visualize bone interstitial fluid space using confocal microscopy. *Bone* **44**, 1015-7 (2009).

105. Bell, K.L. *et al.* Regional differences in cortical porosity in the fractured femoral neck. *Bone* **24**, 57-64 (1999).

106. Schlecht, S.H., Pinto, D.C., Agnew, A.M., Stout, S.D. The effects of disuse on the mechanical properties of bone: what unloading tells us about the adaptive nature of skeletal tissue. *Am. J. Phys. Anthropol.* **149**, 599-605 (2012).

107. Taylor, R. Interpretation of the correlation coefficient: a basic review. *J. Diagn. Med. Sonogr.* 6, 35–39 (1990).

108. Tommasini, S.M., Nasser, P., Jepsen, K.J. Sexual dimorphism affects tibia size and shape but not tissue-level mechanical properties. *Bone* **40**, 498-505 (2007).

ACKNOWLEDGEMENTS

AUTHOR CONTRIBUTIONS

J.J.M. led project and consultation, secured funding, carried out histology lab work, data analysis, wrote first draft of manuscript; H.B. supervised project, interpreted data; M.F. performed aDNA analysis; S.C. performed initial in-silico screening for aDNA; K.N. and E.B. assisted with aDNA lab work; N.R.D.G. and M.M.W. assisted with histology lab work;

1043 L.K. assisted with osteology, led research permissions and consultation, interpreted data; A.P.
1044 secured funding and coordinated the sample collection; C.P. supervised the aDNA data
1045 generation and aDNA analysis; R.L. K. supervised project, secured funding, conducted
1046 osteology, collected samples, interpreted data, organised research permissions and
1047 consultation. All edited the manuscript and gave approval for publication.
1048

1054   **COMPETING INTERESTS**

1055   The authors declare no competing interests.
1056
1057   **ETHICS APPROVAL STATEMENT**
1058
1059 Approval to conduct this research was obtained from the Solomon Islands National Museum.
1060 The analysis and release of data were in consultation with and co-authorship by community
1061 representative (Lawrence Kiko), with whom also a report summarising the findings was filed.
1062 The thin sections will be repatriated to the Solomon Islands National Museum upon the
1063 completion of this project. All research followed ethical guidelines of the American
1064 Association of Biological Anthropologists and the Australasian Society for Human Biology.
1065

1066   **FIGURE LEGENDS**
1067
1068 **Figure 1.** Location of Taumako (red dashed outline), part of the Duff Islands (red marker)

1069 complex in Melanesia. Map was drawn by first author (JJM) using Microsoft Office 365

1070 PowerPoint (version 2207) https://www.microsoft.com/en-au/microsoft-365.

1071
1072 **Figure 2**. Summary of histomorphometric techniques used in this study. From left sketch of

1073 right posterior human femur: a) posterior cortical bone quadrant showing a strip (red dashed

1074 lines) of bone surface examined histologically from which vascular porosity (V.Po) was

1075 collected; b) three intra-cortical regions of interest (black rectangles) contained within the

1076 larger strip examined for osteon population density (OPD), Haversian canal area (H.Ar), and

1077 secondary osteon area (On.Ar); c) bone histology under transmitted light showing Haversian

1078 canals counted for V.Po (white triangle markers) and measured for area (c.1); d) bone

1079 histology under linearly polarised light showing secondary osteon area (d.1). Scale bars in c)–

1080 d) are 200μm.

1081

1082   **Figure 3.** Simple boxplots illustrating differences in vascular porosities adjusted by different

1083   measures of femoral bone size (Circ: circumference of midshaft, Ct.W: cortical width), and

1084   ratio of Haversian canal area to osteon area, compared between the sexes (boxplots a–c), and

1085   age-at-death categories (d–f; where YA: young adults, MA: middle-aged adults, OA: older

1086   adults). ***$p<0.001$ using Mann Whitey *U* test (see Table 3).

1087

1088   **Figure 4.** Montage combining simple correlations between the key histomorphometric

1089   variables examined in this study. We do not show y and x axis values as this figure is

1090   intended as a simple illustrative overview of how well the variables agree with each other.

1091   *$p<0.05$, **$p<0.01$, ***$p<0.001$ using Spearman's *Rho* tests (see Supplementary Information

1092   Table 4).

1093   **TABLES**

1094   **Table 1.** Descriptive summary of gross femoral data sub-divided by estimated sex and age-at-

1095   death. SD: standard deviation, MAX.: maximum, MIN.: minimum, Ct.W_RI: robusticity

1096   index (RI) calculated using cortical width (Ct.W) data, Circ_RI: robusticity index (RI)

1097   calculated using midshaft circumference (Circ). The RI variables are unitless.

GROSS FEMORAL MEASURES						
Sub-divided by sex and age-at-death		**N**	**Min.**	**Max.**	**Mean**	**SD**
FEMALE	Femur max length (cm)	6	40.60	44.50	42.42	15.41
	Circ (mm)	36	69.00	106.00	89.81	7.86
	Ct.W (mm)	36	3.95	13.23	8.77	1.96
	Circ_RI	6	17.93	22.33	20.66	1.91
	Ct_W_RI	6	1.47	2.57	2.08	0.46
MALE	Femur max length (cm)	17	30.40	47.00	42.92	4.70
	Circ (mm)	33	85.00	106.00	95.79	5.53
	Ct.W (mm)	33	6.56	15.27	10.77	1.65
	Circ_RI	17	19.43	34.21	22.85	3.84
	Ct_W_RI	17	1.75	4.16	2.58	0.56
YOUNG ADULT	Femur max length (cm)	16	304.00	477.00	426.81	48.13
	Circ (mm)	34	69.00	106.00	91.29	8.05
	Ct.W (mm)	34	3.95	15.27	9.61	2.21
	Circ_RI	16	17.93	34.21	22.40	4.18
	Ct_W_RI	16	1.47	4.16	2.45	0.67
MIDDLE-AGED ADULT	Femur max length (cm)	2	406.00	421.00	413.50	10.61
	Circ (mm)	13	81.00	106.00	93.15	7.54
	Ct.W (mm)	13	6.64	13.23	9.42	2.07
	Circ_RI	2	21.43	22.33	21.88	0.64
	Ct_W_RI	2	2.43	2.57	2.50	0.10
OLD ADULT	Femur max length (cm)	5	420.00	458.00	437.00	15.31
	Circ (mm)	22	83.00	104.00	94.50	6.15
	Ct.W (mm)	22	6.73	13.03	10.07	1.86
	Circ_RI	5	19.43	23.80	22.05	1.78
	Ct_W_RI	5	2.21	2.78	2.44	0.25

Table 2. Descriptive summary of histology data sub-divided by estimated sex and age-at-death groups. SD: standard deviation, MAX.: maximum, MIN.: minimum, V.Po: density of canals/pores per mm^2, H.Ar/On.Ar: ratio of Haversian canal to osteon area in µm², OPD: osteon population density per mm^2, Ct.W_RI: robusticity index (RI) calculated using cortical width (Ct.W) data, Circ_RI: robusticity index (RI) calculated using midshaft circumference (Circ). All variables are unitless.

FEMUR HISTOLOGY MEASURES						
Sub-divided by sex and age-at-death		N	Min.	Max.	Mean	SD
FEMALE	V.Po/Ct.W	36	1.29	4.42	2.34	0.77
	V.Po/Circ	36	12.86	39.05	22.02	5.80
	H.Ar/On.Ar	9	6.50	10.40	8.31	1.36
	OPD/Ct.W_RI	4	6.34	6.84	6.62	0.24
	OPD/Circ_RI	4	5.53	7.86	6.76	0.53
MALE	V.Po/Ct.W	32	0.83	3.16	1.64	0.49
	V.Po/Circ	32	10.46	33.41	18.34	4.49
	H.Ar/On.Ar	12	4.57	9.46	7.61	1.52
	OPD/Ct.W_RI	8	3.40	6.69	5.31	1.20
	OPD/Circ_RI	9	4.78	7.66	6.34	1.08
YOUNG ADULT	V.Po/Ct.W	33	1.07	4.42	2.02	0.74
	V.Po/Circ	33	12.77	29.11	20.37	4.27
	H.Ar/On.Ar	13	4.57	9.85	7.83	1.40
	OPD/Ct.W_RI	8	3.40	6.69	5.75	1.16
	OPD/Circ_RI	9	4.90	7.66	6.44	0.96
MIDDLE-AGED ADULT	V.Po/Ct.W	13	1.29	3.40	2.22	0.69
	V.Po/Circ	13	13.98	28.19	21.53	4.75
	H.Ar/On.Ar	4	6.50	10.40	8.17	1.83
	OPD/Ct.W_RI	1	6.84	6.84	6.84	n/a
	OPD/Circ_RI	1	7.86	7.86	7.86	n/a
OLD ADULT	V.Po/Ct.W	22	.83	3.33	1.88	0.76
	V.Po/Circ	22	10.46	39.05	19.43	7.37
	H.Ar/On.Ar	4	5.42	9.36	7.92	1.73
	OPD/Ct.W_RI	3	4.04	6.81	5.36	1.39
	OPD/Circ_RI	3	4.78	7.39	6.10	1.30

1115

1116 **Table 3.** All results of inferential analyses comparing femoral size, and statistically

1117 significant results of bone histological markers compared between the sex and age groups.

1118 V.Po: density of canals/pores per mm^2, H.Ar/On.Ar: ratio of Haversian canal to osteon area

1119 in µm², OPD: osteon population density per mm^2, *t*: independent samples *t*-test, *U*: Mann

1120 Whitney *U* test, *H*: Kruskal-Wallis test, **p < 0.01, ***p < 0.001.

1121

| COMPARISONS	Test statistic	n	*p*
Males vs. females			
Circ (mm)	*t* = 3.626	F = 36, M = 33	< 0.001***
Ct.W (mm)	*t* = 4.577	F = 36, M = 33	< 0.001***
Bone histology markers compared between males and females			
V.Po/Ct.W (unitless)	*U* = 249	F = 36, M = 32	<0.0001***
V.Po/Circ (unitless)	*t* = 2.905	F = 36, M = 32	0.005**
H.Ar/On.Ar (unitless)	*U* = 40	F = 9, M = 12	0.345
Bone histology markers compared between age groups			
V.Po/Ct.W (unitless)	*H* = 2.4	Y = 33, MA = 13, O = 22	0.301
V.Po/Circ (unitless)	*H* = 3.278	Y = 33, MA = 13, O = 22	0.194

1122

Figure 1.
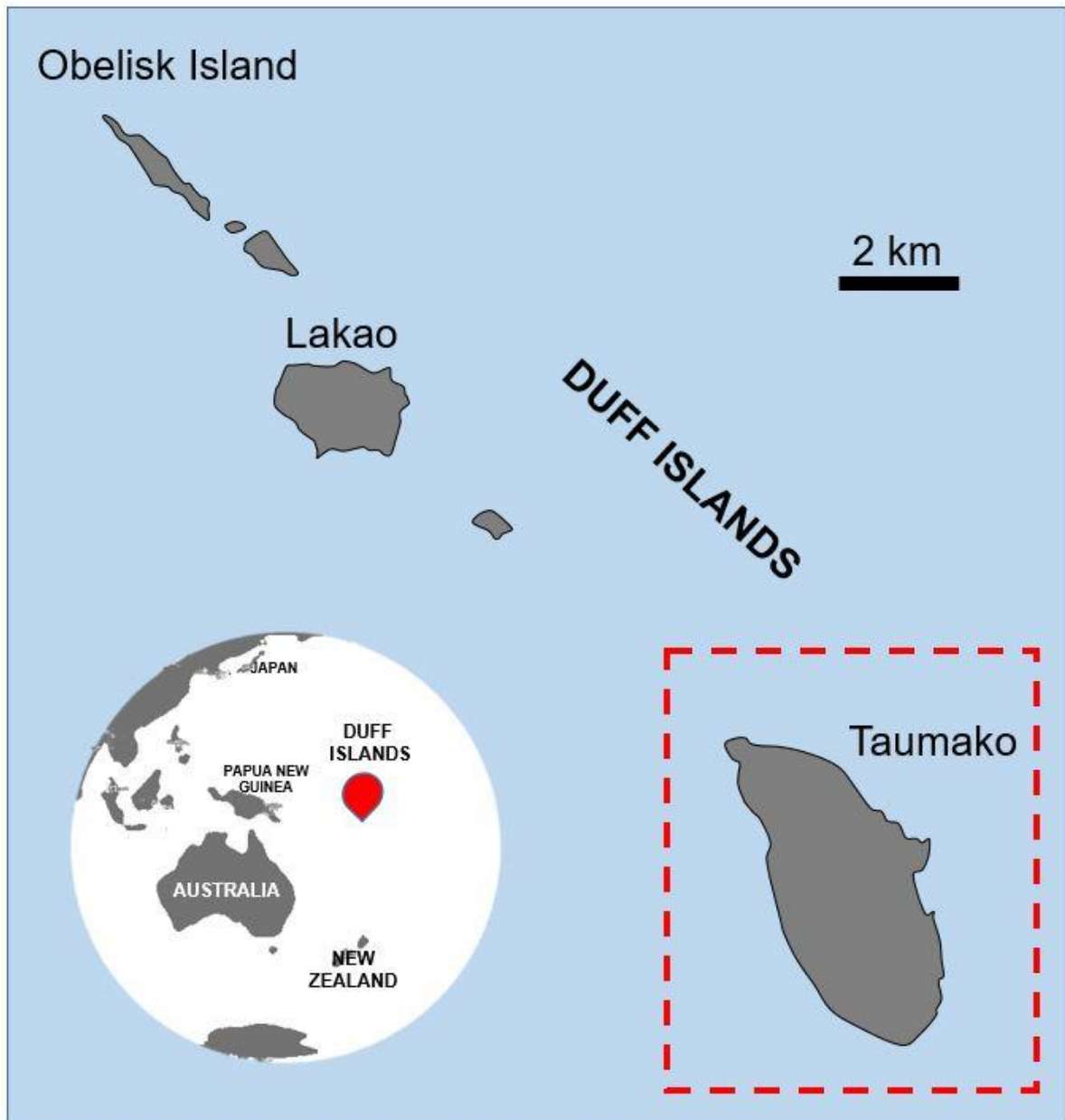
Figure 2.
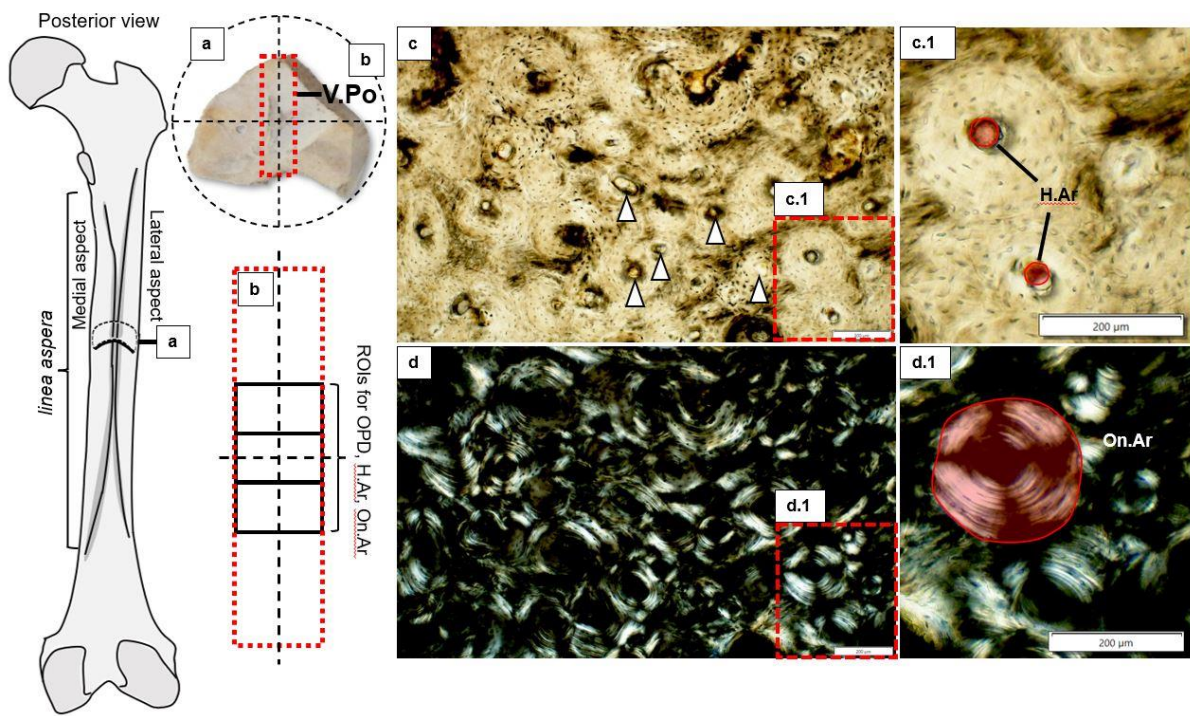
Figure 3.

Differences in vascular porosities with sex and age-at-death
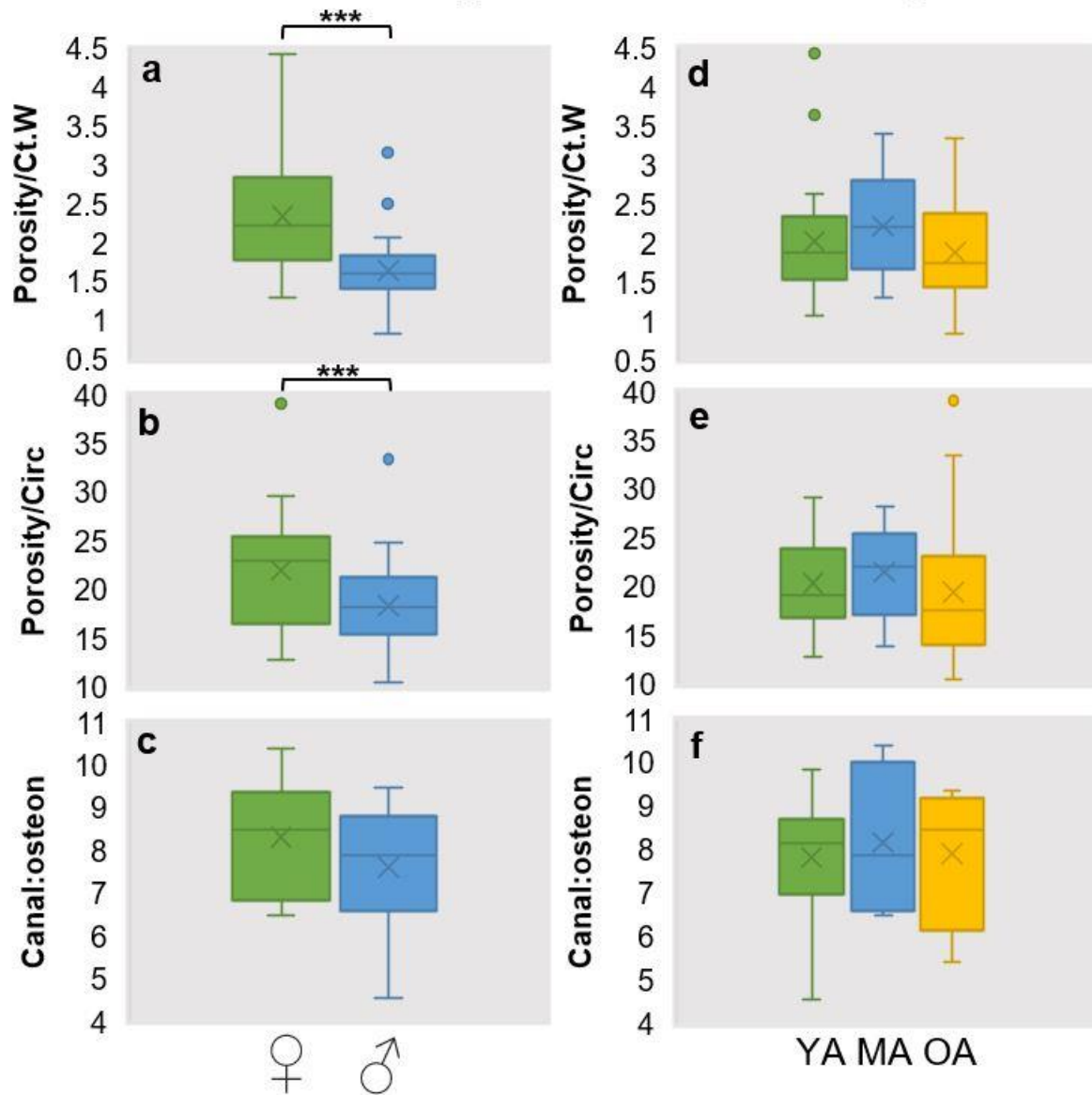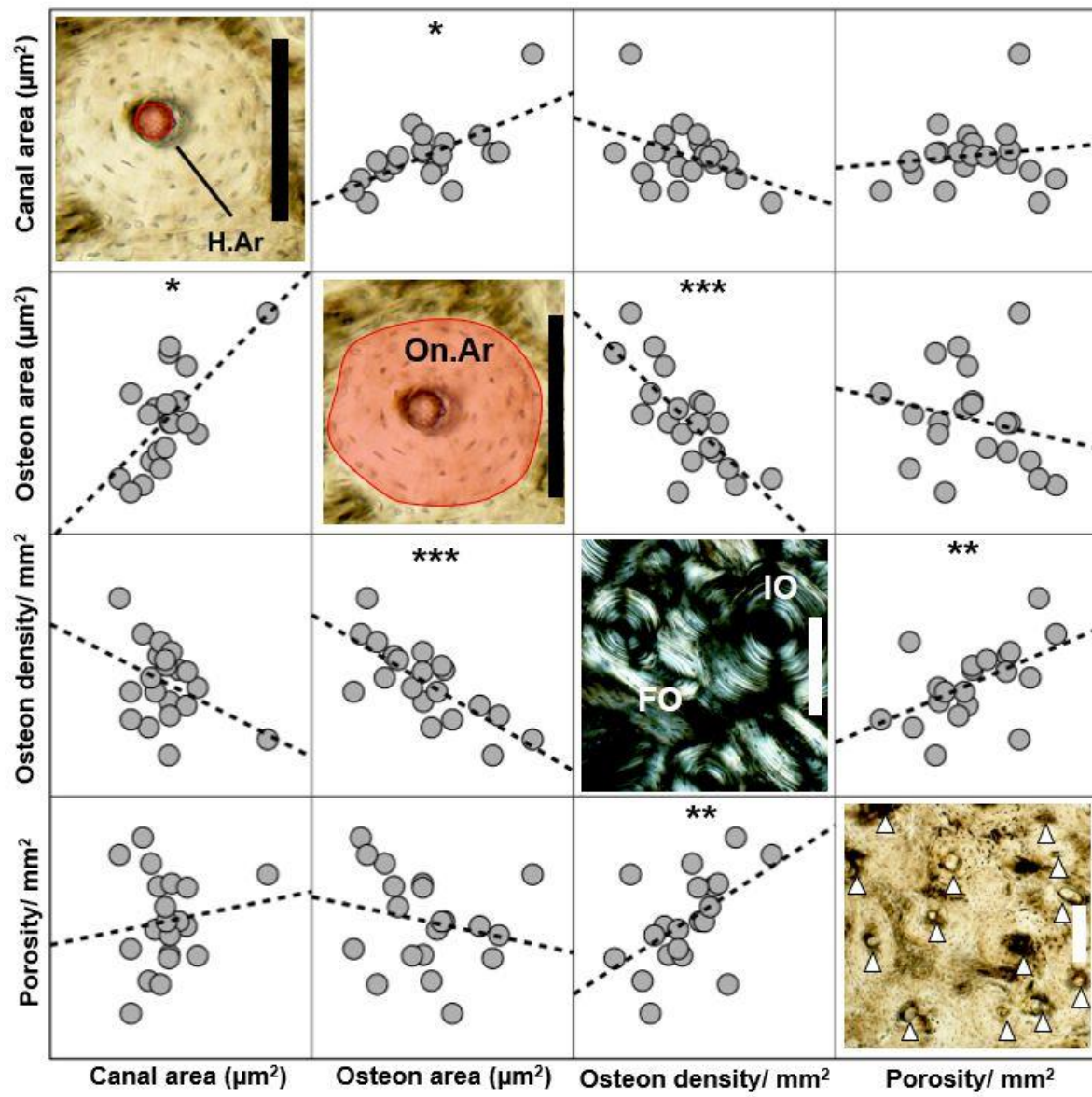
Figure 4.

SUPPLEMENTAL INFORMATION FOR

Female bone physiology resilience in a past Polynesian outlier community

Justyna J. Miszkiewicz[1,2*], Hallie R. Buckley[3], Michal Feldman[4,5,6], Lawrence Kiko[7], Selina Carlhoff[6], Kathrin Naegele[6], Emilie Bertolini[8], Nathalia R. Dias Guimarães[1], Meg M. Walker[1], Adam Powell[9], Cosimo Posth[4,5,6], Rebecca L. Kinaston[3,10,11]

[1]School of Archaeology and Anthropology, Australian National University, Canberra, Australia
[2]School of Social Science, University of Queensland, St Lucia, Australia
[3]Department of Anatomy, Otago School of Biomedical Sciences, University of Otago, Dunedin, New Zealand
[4]Archaeo- and Palaeogenetics Group, Institute for Archaeological Sciences, University of Tübingen, Tübingen, Germany
[5]Senckenberg Centre for Human Evolution and Palaeoenvironment, University of Tübingen, Tübingen, Germany
[6]Department of Archaeogentics, Max Planck Institute for Evolutionary Anthropology, Leipzig, Germany
[7]The Solomon Islands National Museum, Honiara, Solomon Islands
[8]Department of Archaeogentics, Max Planck Institute for the Science of Human History, Jena, Germany
[9]Department of Human Behavior, Ecology and Culture, Max Planck Institute for Evolutionary Anthropology, Leipzig, Germany
[10]Centre for Social and Cultural Research, Griffith University, Queensland, Australia
[11]BioArch South, Waitati, New Zealand

***CORRESPONDENCE**: j.miszkiewicz@uq.edu.au (ORCID: 0000-0002-9769-2706)

SI Table 1. Descriptive summary of data differences between the left and right femora. SD: standard deviation, SE mean: standard error mean.

VARIABLES	FEMUR SIDE	N	MEAN	SD	SE MEAN
Femur length (mm)	Right	14	426.86	43.05	11.50
	Left	9	429.44	39.55	13.18
Midshaft circumference (Circ) (mm)	Right	50	92.32	8.26	1.17
	Left	19	93.58	4.63	1.06
Posterior cortical width (Ct.W) (mm)	Right	50	9.48	2.20	0.31
	Left	19	10.37	1.52	0.35
Vascular porosity (V.Po) adjusted by Ct.W (unitless) (V.Po/Ct.W)	Right	50	2.10	0.78	0.11
	Left	18	1.77	0.52	0.12
V.Po adjusted by Circ (unitless) (V.Po/Circ)	Right	50	20.47	5.75	0.81
	Left	18	19.77	4.87	1.15
Haversian canal:secondary osteon area ratio (H.Ar/On.Ar) (unitless)	Right	14	8.08	1.24	0.33
	Left	7	7.57	1.89	0.72
Osteon population density (OPD) adjusted by Ct.W robusticity index (Ct.W_RI) (OPD/Ct.W_RI)	Right	8	5.87	1.23	0.43
	Left	4	5.50	1.14	0.57
OPD adjusted by Circ robusticity index (Circ_RI) (OPD/Circ_RI)	Right	8	6.39	1.04	0.37
	Left	5	6.59	1.16	0.52
Circ_RI	Right	14	22.48	3.91	1.04
	Left	9	21.97	3.08	1.03
Ct.W_RI	Right	14	2.43	0.65	0.17
	Left	9	2.47	0.45	0.15

SI Table 2. Summary of data differences between the left and right femora tested using an independent samples *t*-test. There were no statistically significant differences in all variables, so both femoral sides were pooled for our analyses. DF: degree of freedom, DIFF.: difference, SE: standard error.

VARIABLES	t	DF	p	MEAN DIFF.	SE DIFF.	95% CONFIDENCE INTERVAL OF THE DIFF.	
						LOWER	UPPER
Femur length mm	-0.145	21	0.886	-2.59	17.84	-39.68	34.51
Circ mm	-0.626	67	0.534	-1.26	2.01	-5.27	2.76
Ct.W mm	-1.606	67	0.113	-0.88	0.55	-1.98	0.21
V.Po/Ct.W	1.640	66	0.106	0.33	0.20	-0.07	0.72
V.Po/Circ	0.463	66	0.645	0.70	1.52	-2.34	3.74
H.Ar/On.Ar	0.743	19	0.466	0.51	0.68	-0.92	1.94
OPD/Ct.W_RI	0.502	10	0.627	0.37	0.74	-1.27	2.01
OPD/Circ_RI	-0.320	11	0.755	-0.20	0.61	-1.56	1.16
Circ_RI	0.329	21	0.745	0.745	0.51	1.54	-2.70
Ct_W_RI	-0.146	21	0.885	0.885	-0.04	0.25	-0.55

EXTENDED DNA METHODS

The DNA processing was conducted in dedicated aDNA facilities at the Max Planck Institute for the Science of Human History, Jena, Germany. For each individual, the dense part within the petrous portion of the temporal bone was drilled for DNA sampling [1]. DNA was extracted from around 50 mg of the sampled powder following published protocols [2]. To prepare the extract for next-generation sequencing a 25-ul aliquot was processed to produce a double-stranded and double-indexed Illumina DNA library following [3, 4]. To prevent that post-mortem deamination damages would be mistaken as authentic sequences in downstream analysis, damage caused by cytosine deamination was partially removed using uracil-DNA glycosylase and endonuclease VIII as described in [5]. Damage was retained in the two terminal positions to be later used for estimating the fraction of deaminated reads [5]. The DNA libraries were subsequently amplified using Herculase II Fusion DNA polymerase according to the manufacturer's protocol. All libraries were directly shotgun single-end sequenced on an Illumina HiSeq 4000 platform ($1 \times 75 + 8 + 8$ cycles). To control for potential laboratory contamination, blank extractions and library preparations were included for each sample batch.

The sequenced reads were binned (demultiplexed) allowing for one mismatch per index. The multiplexed libraries were than processed using the EAGER (v 1.92.54) pipeline [6]. As part of the pipeline, the Illumina adapter sequences were clipped off and the reads were filtered, retaining only reads longer than 30 base pairs using AdapterRemoval (v2.2.0) [8]. The clipped and filtered reads were mapped against the human genome reference hg19 using the BWA aln/samse alignment software (v0.7.12), with a stringency parameter of 0.01, seeding off (-l 16,500), and only retaining reads with Phred-scaled mapping quality scores higher than 30 [8]. Duplicate reads were removed using DeDup v0.12.2 [6]. To authenticate the ancient DNA library, levels of DNA deamination post-mortem damage were measured using mapDamage (v2.0) [9] and compared to the expected values in similar libraries prepared from ancient skeletal elements. Two terminal positions of each fragment were then masked to exclude DNA damage from following analyses [10].

Due to the low number of sequences yielded for each library, the genetic sex was inferred using two independent approaches. Both approaches aim to determine the copy number of each sex chromosome by calculating the number of reads mapping to sex- and autosomal chromosomes. Since genetic females have two copies of the X-chromosome and two copies of each autosomal chromosome, their X-chromosome coverage is expected to be comparable to the autosomal one. However, males have only one copy of the X-chromosome and one of the Y-chromosome and therefore the coverage of each of their sex chromosomes is expected to be half of the autosomal one.

The first method uses the mapping counts across a total of around 1.24 million genome-wide SNPs that were ascertained since they are informative for population history studies [11-13]. However, they can also be useful to estimate genetic sex [14]. For this purpose, the reads mapping to each ascertained position were counted using SAMtools and averaged for each chromosome using an inhouse script [15]. The Y- and the X- chromosome average coverages were each normalized using the average autosomal coverage. Then the normalized Y- and the X- chromosome average coverages were compared and used for the sex assignment.

The second approach was specifically designed for low-covered shotgun genomes and has been shown to confidently estimate genetic sex for libraries with as little as 1,000 mapping reads. In contrast to the first method, here the average coverage is estimated across the entire X- and the entire autosomal- chromosome sequences of the human reference hg19 (and not

on specific positions). The ratio between the X and the autosomal average coverages is calculated and used for the sex assignment as described in [16].

References:

1. Pinhasi, R. *et al.* DNA yields from the inner ear part of the human petrous bone. *PLOS ONE* **10**, e0129102 (2015).
2. Dabney, J. *et al.* Complete mitochondrial genome sequence of a Middle Pleistocene cave bear reconstructed from ultrashort DNA fragments. *Proc. Natl. Acad. Sci. U.S.A.* **110**, 15758–15763 (2013).
3. Meyer, M., Kircher, M. Illumina sequencing library preparation for highly multiplexed target capture and sequencing. *Cold Spring Harb. Protoc.* **2010**, pdb.prot5448 (2010).
4. Kircher, M., Sawyer, S., Meyer, M. Double indexing overcomes inaccuracies in multiplex sequencing on the Illumina platform. *Nucleic Acids Res.* **40**, e3 (2012).
5. Rohland, N., Harney, E., Mallick, S., Nordenfelt, S., Reich, D. Partial uracil–DNA–glycosylase treatment for screening of ancient DNA. *Philos. Trans. R. Soc. Lond. B Biol. Sci.* **370**, 20130624 (2015).
6. Peltzer, A. *et al.* EAGER: Efficient ancient genome reconstruction. *Genome Biol.* **17**, 60 (2016).
7. Schubert, M., Lindgreen, S., Orlando, L. AdapterRemoval v2: Rapid adapter trimming, identification, and read merging. *BMC. Res. Notes* **9**, 88 (2016).
8. Li, H., Durbin, R. Fast and accurate short read alignment with Burrows–Wheeler transform. *Bioinformatics* **25**, 1754–1760 (2009).
9. Jónsson, H., Ginolhac, A., Schubert, M., Johnson, P.L.F., Orlando, L. mapDamage2.0: Fast approximate Bayesian estimates of ancient DNA damage parameters. *Bioinformatics* **29**, 1682–1684 (2013).
10. Jun, G., Wing, M. K., Abecasis, G. R., Kang, H. M. An efficient and scalable analysis framework for variant extraction and refinement from population-scale DNA sequence data. *Genome Res.* **25**, 918-925 (2015).
11. Fu, Q. *et al.* DNA analysis of an early modern human from Tianyuan Cave, China. *Proc. Natl. Acad. Sci. U.S.A.* **110**, 2223–2227 (2013).
12. Haak, W. *et al.* Massive migration from the steppe was a source for Indo-European languages in Europe. *Nature* **522**, 207–211 (2015).
13. Mathieson, I. *et al.* Genome-wide patterns of selection in 230 ancient Eurasians. *Nature* **528**, 499–503 (2015).
14. Fu, Q., *et al.* The genetic history of ice age Europe. *Nature* **534**, 200-205 (2016).
15. Li, H. A statistical framework for SNP calling, mutation discovery, association mapping and population genetical parameter estimation from sequencing data. *Bioinformatics* **27**(21), 2987-2993 (2011).
16. Mittnik, A., Wang, C. C., Svoboda, J., Krause, J. (2016). A molecular approach to the sexing of the triple burial at the Upper Paleolithic Site of Dolní Věstonice. *PloS one*, **11**, e0163019.

SI Table 3 (continues p. 6). Matching of sex results based on gross anatomical methods and those supported by aDNA. There was total n = 69, total n of mismatches = 6, total n of matches = 42, which results in 88% success rate of sex estimation using both methods. aDNA was not available (n/a) for n = 21 individuals.

ID	Estimated sex	Genetic sex approach 1 (all positions; X/auto ratio)	Genetic sex approach 2 (1240K positions; X/Y ratio)	Mismatch
B178	Female	Male	Male	x
B54	Female	Female	Female	
B83	Female	n/a	n/a	n/a
B91	Female	Female	Female	
B13	Female	n/a	n/a	n/a
B140	Female	Female	Female	
B21	Female	Male	Male	x
B48	Female	Male	Male	x
B63	Female	Female_low_certainty	Female	
B115	Female	Female	Female	
B121	Female	Male	Male	x
B150	Female	Female	Female	
B84	Female	Female	Female	
B141	Female	n/a	n/a	n/a
B139	Female	Female	Female	
B3	Female	Female	Female	
B41	Female	n/a	n/a	n/a
B71	Female	n/a	n/a	n/a
B103	Female	Female	Female	
B163	Female	Female	Female	
B159	Female	Female_low_certainty	Female_low_certainty	
B6	Female	n/a	n/a	n/a
B65	Female	Female	Female	
B79	Female	n/a	n/a	n/a
B23	Female	n/a	n/a	n/a
B15	Female	Male	Male	x
B25	Female	n/a	n/a	n/a
B38	Female	n/a	n/a	n/a
B109	Female	Female_low_certainty	Female	
B59	Female	Female	Female	
B152	Female	Female	Female	
B37	Female	n/a	n/a	n/a
B110	Female	Female	Female	
B160	Female	n/a	n/a	n/a
105-1	Female	n/a	n/a	n/a
105-2	Female	n/a	n/a	n/a
B180	Female	Female	Female	
B30	Female	Female	Female	
B45	Female	n/a	n/a	n/a
B95	Female	Female	Female	
B69	Female	Female	Female	

B44	Female	Male	Male	x
B149	Male	Male	Male	
B68	Male	Male	Male	
B195	Male	n/a	n/a	n/a
B108	Male	Male	Male	
B42	Male	Male	Male	
B73	Male	Male	Male	
B85	Male	n/a	n/a	n/a
B126	Male	Male	Male	
B145	Male	Male	Male	
B169	Male	Male	Male	
B148	Male	n/a	n/a	n/a
B177	Male	Male	Male	
B179	Male	Male	Male	
B194	Male	n/a	n/a	n/a
B1	Male	Male	Male	
B181	Male	Male	Male	
B104	Male	Male	Male	
B176	Male	Male	Male	
B189	Male	Male	Male	
B196	Male	Male	Male	
B24	Male	n/a	n/a	n/a
B133	Male	Male	Male	
B87	Male	Male	Male	
B14	Male	Male	Male	
B173	Male	n/a	n/a	n/a
B182	Male	Male	Male	
B22	Male	Male	Male	

SI Table 4. Statistically significant results of correlations of bone histological markers compared between the sex and age-at-death groups. H.Ar: Haversian canal area, On.Ar: osteon area, OPD: osteon population density per mm^2, V.Po: density of canals/pores per mm^2, *Rho*: Spearman's Rho test. $*p < 0.5$, $**p < 0.01$, $***p < 0.001$.

CORRELATIONS	Test statistic	n	*p*
Histology correlations across the sample			
H.Ar and On.Ar	*Rho* = 0.435	21	0.049*
On.Ar and OPD	*Rho* = -0.670	21	<0.001***
V.Po and OPD	*Rho = 0.531*	20	0.016**